Title

Oestrogen receptor beta ligand: a novel treatment to enhance endogenous functional remyelination.

Journal

Brain : a journal of neurology, 133(10)

ISSN

0006-8950

Authors

Crawford, Daniel K
Mangiardi, Mario
Song, Bingbing
et al.

Publication Date

2010-10-01

DOI

10.1093/brain/awq237

Peer reviewed

doi:10.1093/brain/awq237 Brain 2010: 133; 2999–3016 | 2999

BRAIN
A JOURNAL OF NEUROLOGY

Oestrogen receptor β ligand: a novel treatment to enhance endogenous functional remyelination

Daniel K. Crawford,[1,*] Mario Mangiardi,[1,*] Bingbing Song,[3] Rhusheet Patel,[1] Sienmi Du,[1] Michael V. Sofroniew,[2,3] Rhonda R. Voskuhl[1,2] and Seema K. Tiwari-Woodruff[1,2]

1 Multiple Sclerosis Programme, Department of Neurology, School of Medicine, University of California, Los Angeles, CA 90095, USA
2 Brain Research Institute, School of Medicine, University of California, Los Angeles, CA 90095, USA
3 Department of Neurobiology School of Medicine, University of California, Los Angeles, CA 90095, USA

*These authors contributed equally to this work.

Correspondence to: Seema K. Tiwari-Woodruff,
Multiple Sclerosis Program at UCLA,
Department of Neurology,
UCLA School of Medicine,
Neuroscience Research Building 1, 475C,
635 Charles E Young Drive, Los Angeles,
CA 90095-1769, USA
E-mail: seemaw@ucla.edu

Demyelinating diseases, such as multiple sclerosis, are characterized by inflammatory demyelination and neurodegeneration of the central nervous system. Therapeutic strategies that induce effective neuroprotection and enhance intrinsic repair mechanisms are central goals for future therapy of multiple sclerosis. Oestrogens and oestrogen receptor ligands are promising treatments to prevent multiple sclerosis-induced neurodegeneration. In the present study we investigated the capacity of oestrogen receptor β ligand treatment to affect callosal axon demyelination and stimulate endogenous myelination in chronic experimental autoimmune encephalomyelitis using electrophysiology, electron microscopy, immunohistochemistry and tract-tracing methods. Oestrogen receptor β ligand treatment of experimental autoimmune encephalomyelitis mice prevented both histopathological and functional abnormalities of callosal axons despite the presence of inflammation. Specifically, there were fewer demyelinated, damaged axons and more myelinated axons with intact nodes of Ranvier in oestrogen receptor β ligand-treated mice. In addition, oestrogen receptor β ligand treatment caused an increase in mature oligodendrocyte numbers, a significant increase in myelin sheath thickness and axon transport. Functional analysis of callosal axon conduction showed a significant improvement in compound action potential amplitudes, latency and in axon refractoriness. These findings show a direct neuroprotective effect of oestrogen receptor β ligand treatment on oligodendrocyte differentiation, myelination and axon conduction during experimental autoimmune encephalomyelitis.

Keywords: oligodendrocytes; remyelination; myelin sheath; EAE; neurodegeneration; neuroprotection

Abbreviations: DAPI = 4′,6-diamidino-2-phenylindole; EAE = experimental autoimmune encephalomyelitis; ERβ = oestrogen receptor β; GFAP = glial fibrillary acidic protein; GST-pi = glutathione-S transferase-pi; NF200 = neurofilament 200; PDGFR-α = platelet-derived growth factor receptor-α; PLP-EGFP = proteolipid protein-enhanced green fluorescent protein

Received April 2, 2010. Revised June 13, 2010. Accepted July 8, 2010

Introduction

Inflammatory infiltration and demyelination of the CNS leading to axonal loss and neurological impairments are hallmarks of multiple sclerosis and experimental autoimmune encephalomyelitis (EAE) (Lassmann *et al.*, 2007; Trapp and Nave, 2008). Despite the ability of the adult brain to generate oligodendrocytes with myelination capacity, remyelination in multiple sclerosis and EAE are incomplete (Lassmann *et al.*, 1997; Chang *et al.*, 2002; Frischer *et al.*, 2009). Current anti-inflammatory or immunomodulatory treatments, while partially effective in the relapsing stage of the disease, have only modest-to-minimal effects on the development of neurodegeneration and clinical disability in the secondary progressive phase of disease (Molyneux *et al.*, 2000; Filippi *et al.*, 2002). Therefore, it is important to find novel treatments that could prevent demyelination and/or enhance remyelination.

EAE is used to understand neurodegenerative mechanisms that occur in the setting of immune-mediated demyelination (Bannerman *et al.*, 2005; Steinman and Zamvil, 2006; Jones *et al.*, 2008). EAE has been extensively used to address immune mechanisms of currently approved drugs for multiple sclerosis (Gasperini and Ruggieri, 2009) and to screen various compounds including oestrogens as future therapeutic drugs (Tiwari-Woodruff and Voskuhl, 2009). Oestrogen-based treatments are promising as neuroprotective agents in multiple sclerosis due to the fact that oestrogen is known to be neuroprotective in other diseases, including spinal cord injury (Sribnick *et al.*, 2005; Chaovipoch *et al.*, 2006), stroke (Dubal *et al.*, 2006; Wang *et al.*, 2009), Alzheimer's disease (Yue *et al.*, 2005; Wilson *et al.*, 2006), Parkinson's disease (Xu *et al.*, 2006; Quesada *et al.*, 2008), amyotrophic lateral sclerosis (Groeneveld *et al.*, 2004) and acoustic trauma (Meltser *et al.*, 2008). A multicentre clinical trial is currently underway using oestriol treatment in female patients with multiple sclerosis.

Our investigations in EAE have shown differential effects of oestrogen receptor α ligand treatment, which reduced CNS inflammation versus oestrogen receptor β ligand treatment, which preserved axon and myelin despite having no effect on CNS inflammation in spinal cords (Morales *et al.*, 2006; Tiwari-Woodruff *et al.*, 2007; Tiwari-Woodruff and Voskuhl, 2009). In light of this putative direct neuroprotective effect of oestrogen receptor β ligand treatment in EAE, it was of interest to investigate its ability to affect the primary targets of the EAE/multiple sclerosis pathological process: oligodendrocytes, myelin and axons.

EAE has generally been thought to predominantly target the spinal cord, leading to sensory and motor impairments, while multiple sclerosis targets both the brain and spinal cord, and results in a variety of impairments including sensorimotor, cognitive and difficulty with information processing. However, recently it was recognized that EAE may involve other CNS structures (Hobom *et al.*, 2004; Wensky *et al.*, 2005; Brown and Sawchenko, 2007; Rasmussen *et al.*, 2007; MacKenzie-Graham *et al.*, 2009; Ziehn *et al.*, 2010). In the present study, we investigated the possible therapeutic effect of oestrogen receptor β ligand treatment on EAE-induced decreases in oligodendrocyte numbers and demyelination, as well as decreases in axon-conduction and axon-transport deficits in the corpus callosum. The corpus callosum is a critical white matter structure that is impacted early in the course of multiple sclerosis and corpus callosum abnormalities are associated with fatigue, motor impairment and cognitive changes (Manson *et al.*, 2006, 2008; Bonzano *et al.*, 2008). Integrity of the corpus callosum in multiple sclerosis reflects both discrete white matter lesions and diffuse normal-appearing white matter changes, making it a potentially useful surrogate marker of clinically significant brain abnormalities in multiple sclerosis (Boroojerdi *et al.*, 1998; Ozturk *et al.*, 2001; Warlop *et al.*, 2008).

We report here that oestrogen receptor β ligand treatment during EAE stimulated an increase in the mature myelinating oligodendrocyte population and increased myelin thickness, thereby decreasing axon damage, ameliorating callosal axon conduction and improving axon transport deficits. This is the first description of an agent that can be neuroprotective in the setting of inflammation in the EAE model.

Materials and methods

Animals

Breeding pairs of proteolipid protein-enhanced green fluorescent protein (PLP-EGFP) transgenic mice in the C57BL/6J background were a kind gift from Dr Wendy Macklin (University of Colorado, Denver, CO, USA). The generation, characterization and genotyping of PLP-EGFP transgenic mice have been reported previously (Fuss *et al.*, 2001; Mallon *et al.*, 2002). Mice were bred in-house at the University of California, Los Angeles animal facility. All procedures were conducted in accordance with the National Institutes of Health and were approved by the Animal Care and Use Committee of the Institutional Guide for the Care and Use of Laboratory Animals at University of California, Los Angeles.

Reagents

Diarylpropionitrile was purchased from Tocris Bioscience (Ellisville, MO). Miglyol 812 N liquid oil was obtained from Sasol North America (Houston, TX). Myelin oligodendrocyte glycoprotein, amino acids 35–55, was synthesized to >98% purity by Mimotopes (Clayton, Victoria, Australia).

Hormone manipulations

Female mice (6-weeks-old) were ovariectomized two weeks prior to induction of EAE. Ovariectomized mice were treated with subcutaneous injections of diarylpropionitrile at 8 mg/kg per day or vehicle (10% ethanol and 90% Migylol) every other day beginning 7 days before EAE induction and throughout the entire disease duration. The diarylpropionitrile dose was chosen based on uterine weight measurements for biological response and on previous EAE experiments using this compound (Tiwari-Woodruff *et al.*, 2007).

Experimental autoimmune encephalomyelitis induction

We have routinely induced chronic EAE in female C57BL/6 mice (Morales *et al.*, 2006; Tiwari-Woodruff *et al.*, 2007). Transgenic PLP-EGFP mice immunized with myelin oligodendrocyte glycoprotein show a similar disease course. On post-inoculation Day 0 (and again on Day 7), each mouse received subcutaneous inoculation with both myelin oligodendrocyte glycoprotein peptide 35–55 (300 μg/mouse) in CFA H37 Ra (1 mg/ml *Mycobacterium tuberculosis* H37 Ra) and an intraperitoneal inoculation of *Bordatella pertussis* toxin (500 ng/mouse). A second inoculation of *B. pertussis* toxin was administered on post-inoculation Day 2. Mice were monitored and scored daily for clinical disease severity according to the standard 0–5 EAE grading scale: 0 = unaffected; 1 = tail limpness; 2 = failure to right upon attempt to roll over; 3 = partial hindlimb paralysis; 4 = complete hindlimb paralysis and 5 = moribund. EAE clinical signs began at Days 9–10. Mice were sacrificed at either Day 20 or Day 36 after disease induction.

Number of mice

There were usually three different treatment ovariectomized groups (normal, vehicle + EAE and oestrogen receptor β ligand + EAE) per experiment. To assess the effect of ovariectomy in PLP-EGFP C57BL/6 mice we used intact mice (normal, vehicle + EAE and oestrogen receptor β ligand + EAE). There were 10 animals per treatment group (four animals for electrophysiology recording, three animals perfused for immunohistochemistry and three animals perfused for electron microscopy). The experiment was repeated three times.

Histopathology, immunohistochemistry and electron microscopy

Perfusion-fixed brain slices and immunohistochemistry

Paraformaldehyde-fixed consecutive sections (Tiwari-Woodruff *et al.*, 2007; Crawford *et al.*, 2009*b*) were examined by immunohistochemistry and various series of cell-type-specific antibodies were used. To detect axons: anti-Neurofilament 200 (NF200; 1:500, Chemicon and 1 : 1000, Sigma); injured axons: anti-β-amyloid precursor protein (1:500, Abcam, Cambridge, MA); astrocytes: anti-glial fibrillary acidic protein (GFAP; 1 : 1000, Chemicon); oligodendrocyte progenitors: anti-platelet-derived growth factor receptor-α (PDGFR-α; 1:500, Chemicon) and anti-olig2 (1:500, Chemicon); mature oligodendrocytes: anti-glutathione S transferase-pi (GST-pi; 1:1000, Chemicon) and PLP-EGFP fluorescence; myelin: anti-myelin basic protein (1:1000, Chemicon); microglia/macrophage/monocyte: anti-CD45 (1:1000; PharMingen, La Jolla, CA); macrophages: Mac3 (1:500; BD Biosciences, San Diego, CA); T cells: anti-CD3 (1:1000, Abcam); nodal proteins: Caspr, Nav1.6, Kv1.2 (Alomone Labs, Jerusalem, Israel and Antibodies Inc, Davis, CA) were used. The second antibody step was performed by labelling with antibodies conjugated to TRITC and Cy5 (1:1000, Vector Labs Burlingame, CA and Chemicon). Immunoglobulin G (IgG) control experiments were performed for all primary antibodies and no staining was observed under these conditions. To assess the number of cells, a nuclear stain 4′,6-diamidino-2-phenylindole (DAPI; 2 ng/ml; Molecular Probes) was added for 15 min prior to final washes after secondary antibody addition. The sections were mounted on slides, dried and coverslipped in fluoromount G (Fisher Scientific, Pittsburgh, PA).

Electron microscopy

Paraformaldehyde- and glutaraldehyde-perfused brains were cut in half sagittally. The genu area of the corpus callosum was identified under a dissecting microscope and 4 mm^2 blocks [from the mid-corpus callosum up to one-third of the splenum, corresponding to the corpus callosum area of Plate 29-48 from the atlas of Franklin and Paxinos (2001)] were carefully dissected. These blocks were further cut into 1 mm sections for Epon embedding.

Tract tracing

PLP-EGFP (normal, vehicle-treated and oestrogen receptor β ligand-treated EAE) mice were anaesthetized with isoflurane and then mounted in a stereotaxic apparatus on Days 28–29 post EAE induction. A small craniotomy was made to expose the area above the targeted region. A glass micropipette (35-μm tip) containing tetramethylrhodamine dextran amine (5%, 10 kDa; Invitrogen) was lowered using stereotaxic coordinates. After a survival time of 7 days (on Days 35–36), animals were euthanized with isoflurane and perfused transcardially with saline followed by 4% paraformaldehyde. Brain and spinal cord sections were co-immunostained and imaged.

Microscopy and quantification

Immunostained brain sections were divided into rostral (hippocampus absent) and caudal slices (hippocampus present), examined and photographed using a spinning disc confocal fluorescent microscope (BX62 DSU; Olympus, Tokyo, Japan) equipped with Plan Fluor objectives, connected to a camera (Hamamatsu Orca). Digital images were acquired separately (at ×10, × 40 or × 60) from delineated corpus callosum regions and analysed using Slide book and ImageJ (NIH). When showing multiple staining, green pseudo-colour was used to represent TRITC-labelled protein (without showing the PLP-EGFP-green channel; e.g. Fig. 7A, Caspr-TRITC shown in red and Nav1.6-Cy5 shown in green). Image intensities were adjusted evenly for each set. Images were captured from the same areas of the corpus callosum using similar light exposure time from delineated regions and quantified as previously shown (Morales *et al.*, 2006; Crawford *et al.*, 2009*b*). Briefly, out of 8–10 optical images acquired for each brain section, every third optical section image was used for analysis. Fluorescent coloured images were separated into individual colours and converted to binary images, manually thresholded and segmented using ImageJ (v1.41 http://rsb.info.nih.gov/ij/). A grid of bin dimensions of 200 × 200 μm was laid on the image and cells (or Caspr protein pairs) in at least five squares per optical section and total numbers of cells (and Caspr nodal pairs and axons) were counted. Similarly myelin (MBP^+), astrocyte ($GFAP^+$) and axon damage (β-amyloid precursor $protein^+$) were analysed by intensity measurement with ImageJ. A fixed threshold range of 0–160 was chosen to highlight the staining signals in normal corpus callosum and all other images were set to this threshold. The total area within this range was measured, averaged, compared and presented (numbers/0.1–0.4 mm^2). For electron microscopic quantification, serial ultrathin sections embedded in Epon were stained with uranyl acetate-lead citrate and analysed in a similar manner to that previously described (Crawford *et al.*, 2009*b*). The ratio of axon diameter to total fibre diameter ('*g* ratio') was measured by dividing the circumference of an axon without myelin by the circumference of the same axon including myelin (Tiwari-Woodruff *et al.*, 2007). For most axons, two encounters were measured. At least 500 axons were analysed in each treatment group.

Electrophysiological recording procedures

Compound action potential recordings, conduction-velocity measurements and axon-refractoriness measurements were performed as previously described (Crawford *et al.*, 2009*a*, *b*). Briefly, each mouse was anaesthetized with isoflurane, decapitated and the brain rapidly removed. Coronal slices that were 400-μm thick were cut in ice-cold artificial cerebrospinal fluid with a vibrating-knife microtome (Leica, model VT1000S, Wetzlar, Germany). Slices were then transferred to a holding chamber containing oxygenated artificial cerebrospinal fluid at room temperature and were allowed to equilibrate under these conditions for at least 1 h prior to recording. The artificial cerebrospinal fluid contained (in mM): NaCl 124, KCl 5, NaH_2PO_4 1.25, $NaHCO_3$ 26, $MgSO_4$ 1.3, $CaCl_2$ 2, glucose 10; pH 7.4; saturated with a 95% O_2/5% CO_2 gas mixture.

Brain slices corresponding approximately to Plates 29–48 in the atlas of Paxinos and Franklin (2001) (Fig. 8A) were used for electrophysiology recording, as previously described (Crawford *et al.*, 2009*b*). Stimulation used for evoked compound action potentials was constant current stimulus-isolated square wave pulses. For analyses of the compound action potential amplitude, standardized input–output functions were generated for each slice by varying the intensity of stimulus pulses (200 μs duration, delivered at 0.2 Hz) in steps from approximately threshold level to an asymptotic maximum (0.3–4.0 mA) for the short-latency negative compound action potential component. To enhance the signal-to-noise ratio, all quantitative electrophysiological analyses were conducted on waveforms that were the average of four successive sweeps. Evoked callosal compound action potential field potentials were amplified and filtered (bandpass = DC to 10 kHz) using an Axopatch 200A amplifier (Molecular Devices, Sunnyvale, CA), digitized at 200 kHz and stored on disk for offline analysis.

Conduction velocity

Corpus callosum conduction velocity can be estimated by changing the distance between the stimulating and recording electrodes from 0.5 to 2.5 mm, while holding the stimulus intensity constant as previously described (Crawford *et al.*, 2009*b*). Recordings are performed using the protocol described above for standard compound action potential measurements. For analysis, the peak latency of the N1 and N2 components are measured at each point and graphed versus this distance. Linear regression analysis can then be performed for each compound action potential component to yield a slope that is the inverse of the velocity, followed by statistical comparison of the velocities.

Axon refractoriness

Axon refractoriness is defined as the reduced excitability of an axon following an action potential. Axon damage can modify refractoriness and its measurement represents a diagnostic tool to measure axon health. To quantify refractoriness, the suppression of a second compound action potential response in paired stimulus trials is determined as previously described (Reeves *et al*., 2005; Crawford *et al*., 2009*a*). Initially, a single stimulating pulse is given at a defined strength to establish a control response (C1). Following this response, two pulses of equal intensity and duration are generated that are separated by a variable time window, starting with an interpulse interval of 8 ms and decreasing in 0.5 ms steps down to 1.5 ms. For analysis, the control response is subtracted from the paired stimulus responses at each interpulse interval. This results in the response, which can be attributed to the second pulse (C2). The estimated N1 and N2 responses for C2 are then measured. Refractoriness is calculated for both N1 and N2 by dividing these C2 compound action potential component amplitudes by their respective C1 compound action potential amplitudes and multiplying by 100%. The results are then graphed versus the interpulse interval and analysed using non-linear regression analysis, with specific use of the Boltzmann sigmoid function. The interpulse interval that results in a 50% reduction in the compound action potential component is then used as a standard measure when making statistical comparisons between groups.

Statistical analysis

Quantification of immunostaining results was similar to previous studies (Tiwari-Woodruff *et al.*, 2007; Crawford *et al.*, 2009*b*). At least six caudal sections from brains electrophysiologically recorded from (two sections each from $n = 3$–5 mice) and 16 mid-to-caudal corpus callosum sections from perfusion-fixed brain (four sections from $n = 4$ mice) were immunostained for a total of 18–22 sections per treatment group. At least 8–10 sections were analysed. To quantify electrophysiology results from each treatment group, recordings from two to three caudal slices ($n = 4$–8 mice) for a total of 8–16 recordings were analysed. For electron microscopy, >500 axons from 8 to 10 random caudal area fields per animal at ×4800 and ×14 000 were used to quantify the '*g* ratio'. Results from the same experimental protocols were pooled together and expressed as mean ± SEM, with n = number of animals. Statistical analysis of mean values was carried out using ANOVA and Friedman Test (only for clinical scores) or Bonferroni's multiple comparison post test. Differences were considered significant at the $P < 0.05$ level. Statistics were performed using Microcal Origin (Northampton, MA) or Prism 4 (GraphPad Prism Software Inc., La Jolla, CA).

Results

Treatment reduces clinical disease-severity scores in experimental autoimmune encephalomyelitis

To visualize and characterize oestrogen receptor β ligand treatment effects on demyelination and axon degeneration, active EAE was induced in PLP-EGFP transgenic C57BL/6 mice (Mallon *et al.*, 2002). To obtain a steady level of oestrogen receptor β ligand, a diarylpropionitrile dose of 8 mg/kg per day (Carswell *et al.*, 2004), oestrogen receptor β ligand or vehicle treatment was administered in ovariectomized mice every other day, starting 1 week prior to active EAE induction. Ovariectomized mice showed similar EAE disease time course and clinical scores as intact animals (Supplementary Fig. 1A). Oestrogen receptor β ligand treatment during EAE had no significant effect early on, that is prior to Day 20, but thereafter demonstrated a significant protective effect throughout the later stages of disease, $P < 0.001$ (Fig. 1A). These results are consistent with our previous findings that treatment with an oestrogen receptor β ligand is clinically protective only during the later phase of the disease (Tiwari-Woodruff *et al.*, 2007).

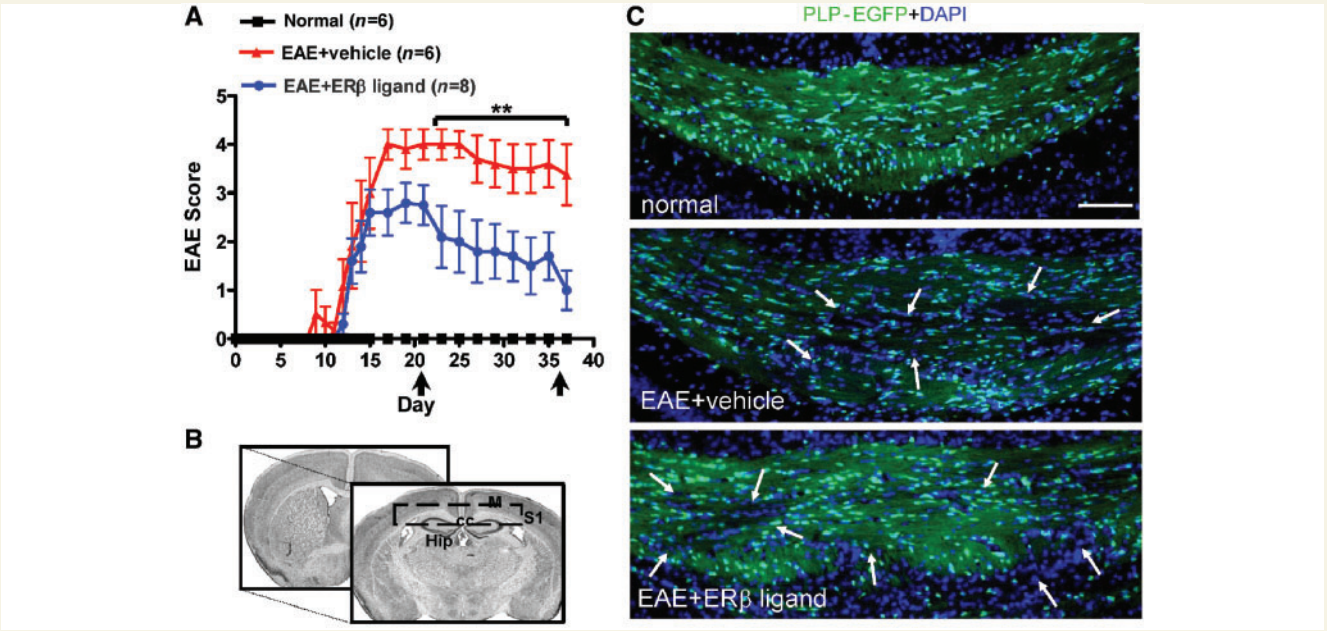

Figure 1 Treatment with oestrogen receptor β ligand significantly improves disease in late chronic EAE. (**A**) Ovariectomized PLP-EGFP C57BL/6 female mice were given subcutaneous injections of diarylpropionitrile, an oestrogen receptor β (ERβ) ligand, during active EAE and scored using the standard EAE grading scale. Oestrogen receptor β ligand-treated mice, compared with vehicle-treated mice, were not significantly different early in disease (up to Day 20 after disease induction), but then became significantly improved later during EAE, (starting at Days 22–25 after disease induction, $^{**}P<0.001$, ANOVA Friedman test). Normal mice did not show any disease and their clinical scores remained zero throughout the experiment. Data are representative of experiments repeated three times. (**B**) Brain slices for immunohistochemistry corresponded approximately to Plates 29–48 in the atlas of Franklin and Paxinos (2001). (**C**) Representative PLP-EGFP expressing (green) and DAPI nuclei (blue) stained corpus callosum sections (×10 magnification) from normal (healthy control), vehicle-treated EAE and oestrogen receptor β ligand-treated EAE mice all sacrificed at Day 36 (late) post disease induction. Compared to normal controls, the corpus callosum of vehicle-treated EAE and oestrogen receptor β ligand-treated EAE had an increase in the total number of infiltrating cells (represented by $DAPI^+$ cells) after induction of EAE. This was accompanied by a reduction in $PLP\text{-}EGFP^+$ cells, as well as PLP-EGFP white matter intensity (white arrows). Scale bar is 100 μm. CC = corpus callosum; Hip = hippocampus; M = motor cortex; S1 = somatosensory cortex.

Inflammation and reactive astrocytosis in the corpus callosum of mice with experimental autoimmune encephalomyelitis

The corpus callosum that connects both cerebral hemispheres is by far the largest fibre tract in the brain and is preferentially involved in multiple sclerosis (Ozturk *et al.*, 2001; Warlop *et al.*, 2008). It is widely believed that rodent EAE rarely affects the brain and is mostly limited to pathology of the spinal cord. Contrary to this belief, we have discovered extensive callosal and cortical pathology, in addition to spinal cord pathology, of both intact and ovariectomized EAE mice (Supplementary Figs 1 and 2). PLP-EGFP fluorescing green cells and myelin in the corpus callosum (delineated region in Fig. 1B) stained with the nuclear stain DAPI allowed us to easily visualize inflammatory and demyelinating lesions in the callosal white matter (arrows in Fig. 1C) and thoracic spinal cord (Supplementary Figs 1B and 2). Demyelinating lesions in vehicle-treated EAE lacked normal expression of PLP-EGFP oligodendrocytes and myelin tracts, whereas in oestrogen receptor β ligand-treated EAE, the corpus callosum and spinal cord indicated increased numbers of PLP-EGFP oligodendrocytes and myelinated tracts along with pockets of infiltrating DAPI nuclei (arrows in Fig. 1C and Supplementary Figs 1 and 2).

Similar to inflammatory cells seen in the spinal cord from EAE mice (Supplementary Fig. 2), the corpus callosum of early and late vehicle-treated EAE mice had many $CD45^+$ cells with activated microglia morphology, along with $Mac3^+$ macrophage and $CD3^+$ T lymphocytes surrounding lesions and vessels (Fig. 2A showing only the late time point). In addition, there was a marked increase in the immunoreactivity intensity of $GFAP^+$ astrocytes in vehicle-treated EAE animals (Fig. 2A). Oestrogen receptor β ligand treatment did not reduce inflammatory cells or reactive astrocyte levels (Fig. 2A). Quantitative analysis of $CD45^+$, $Mac3^+$, $CD3^+$ and $GFAP^+$ cells showed a significant increase in the corpus callosum of vehicle-treated EAE compared to normal that was also observed in EAE mice treated with oestrogen receptor β ligand (Fig. 2B).

Oestrogen receptor β ligand treatment during experimental autoimmune encephalomyelitis maintains a robust oligodendrocyte population

To address the possible cause of the improved state of PLP-EGFP cells and myelin tracts in oestrogen receptor β ligand-treated EAE mice, cells of oligodendrocyte lineage were quantified in the delineated corpus callosum. The PLP-EGFP fluorescent oligodendrocyte population in the corpus callosum of vehicle-treated EAE mice showed patches of decreased intensity, retracted cell processes and smaller cell bodies [Figs 2A, 3A(i) and 3A(ii)] compared to normal mice. Oestrogen receptor β ligand-treated EAE mice had increased numbers of highly processed cells with normal-sized cell bodies [Figs 2A, 3A(i) and (ii)]. Quantification of PLP-EGFP$^+$ cells indicated a significant decrease in the corpus callosum of vehicle-treated EAE mice compared to normal controls. In contrast, PLP-EGFP$^+$ cell numbers in oestrogen receptor β ligand-treated EAE mice were not decreased (Fig. 3B).

The PLP-EGFP cell populations in the corpus callosum are a mixture of oligodendrocyte progenitors and mature oligodendrocyte (Mallon *et al.*, 2002). Therefore, we quantified oligodendrocyte progenitors by immunostaining with olig2 or PDGFR-α antibody and did not observe significant differences between vehicle- and oestrogen receptor β ligand-treated groups (Fig. 3A and B). The mature oligodendrocyte population was quantified by counting cells that express the mature oligodendrocyte marker, glutathione-S transferase-pi (GST-pi). Compared to normal mice, the corpus callosum of vehicle-treated EAE mice had ~25% fewer GST-pi$^+$ cells. In contrast, oestrogen receptor β ligand-treated EAE mice had significantly more

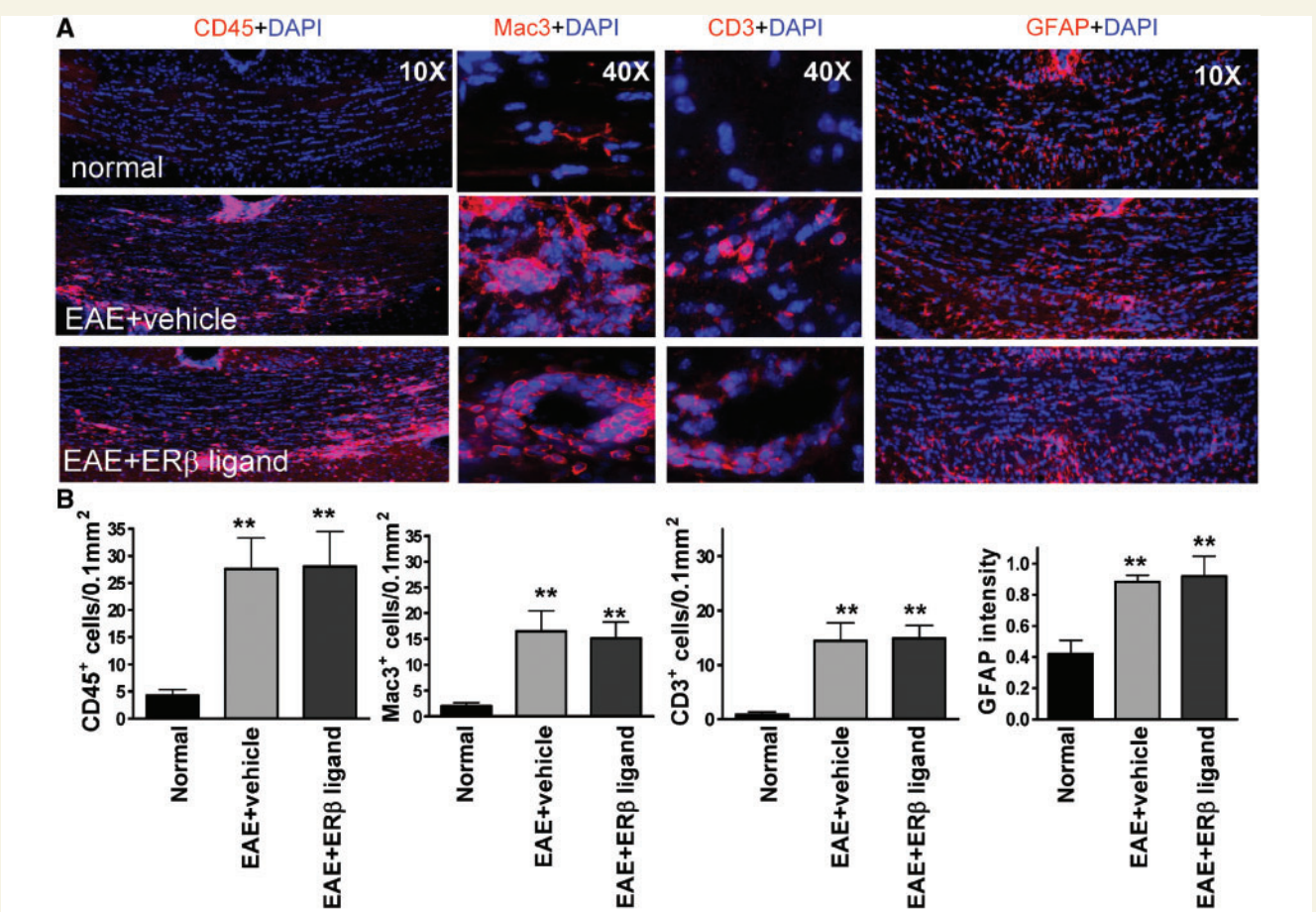

Figure 2 Treatment with oestrogen receptor β ligand did not reduce inflammation or reactive astrocytosis in the corpus callosum of mice with EAE. (**A**) Consecutive corpus callosum sections were also immunostained with antibodies against the common leukocyte antigen-CD45 (red, at ×10 magnification), the macrophage-Mac3 (red, at ×40 magnification), the T cell-CD3 (red, at ×40 magnification) or the astrocyte marker glial fibrillary acidic protein (red, at ×10 magnification). Shown are images from normal control, vehicle-treated EAE and oestrogen receptor β ligand-treated EAE corpus callosum at Day 36 after disease induction. Vehicle-treated EAE and oestrogen receptor β ligand-treated corpus callosum had large areas of CD45$^+$, Mac3$^+$ and CD3$^+$ cells in the corpus callosum as compared to the normal control, as well as large areas of hypertrophic-reactive GFAP$^+$ astrocytes. (**B**) Quantification of number of CD45$^+$, Mac3$^+$ and CD3$^+$ cells and the relative fluorescence intensity of glial fibrillary acidic protein immunostaining demonstrated an increase in both vehicle-treated EAE and oestrogen receptor β ligand-treated EAE as compared to normal mice. Statistically significant compared to normal (**$P < 0.001$ ANOVAs; Bonferroni's multiple comparison post test; $n = 8$–10 mice in each treatment group).

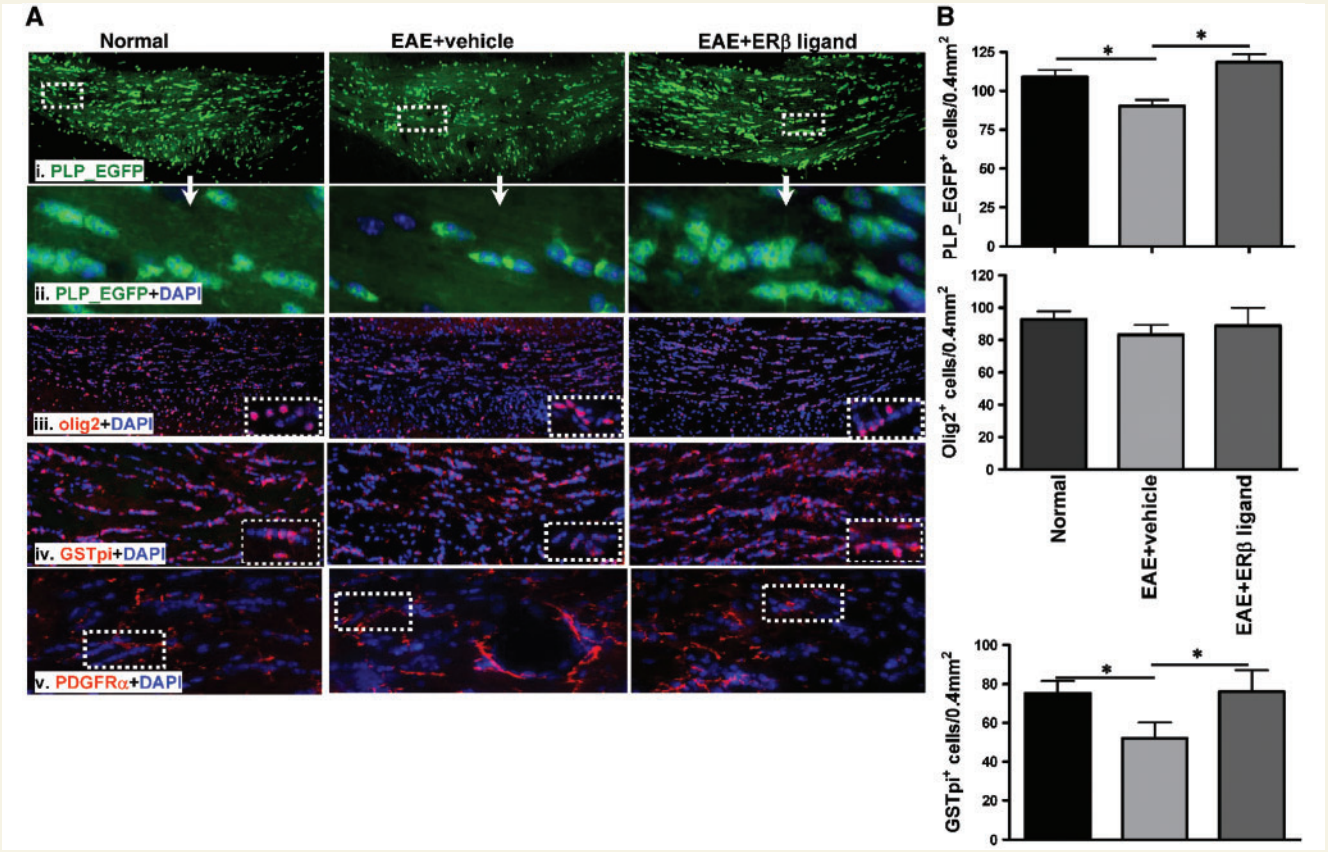

Figure 3 Treatment with an oestrogen receptor β ligand preserved mature myelinating oligodendrocytes in corpus callosum of mice with EAE. (**A**) Representative corpus callosum sections with PLP-EGFP$^+$ cells (green) from normal, vehicle-treated and oestrogen receptor β ligand-treated EAE mice all sacrificed at Day 36 (late) post disease induction [(i) ×10 magnification, (ii) ×40 magnification of the white dashed boxes in panel (i)]. Compared with the corpus callosum of vehicle-treated EAE mice, the number of PLP-EGFP$^+$ cells was significantly increased in oestrogen receptor β ligand-treated EAE. PLP-EGFP$^+$+DAPI$^+$ cells had more processes and were in clusters of >3 cells in oestrogen receptor β ligand-treated corpus callosum compared to cells that were smaller and with fewer processes in vehicle-treated EAE corpus callosum. Consecutive brain slices were also immunolabelled with olig2 (red) +DAPI or GST-pi (red) +DAPI [(iii) (iv) ×10 magnification, inset ×40 magnification]. Olig2$^+$ cell density under all three conditions showed no obvious difference (iii). The GST-pi$^+$ mature oligodendrocyte cell population decreased in vehicle-treated EAE compared to normal control corpus callosum. There is a dramatic increase in the GST-pi cell population in oestrogen receptor β ligand-treated EAE corpus callosum. PDGFRα (red) is a specific marker for oligodendrocyte progenitors. Similar to olig2, PDGFRα$^+$ oligodendrocyte progenitors did not show a significant difference among normal, vehicle-treated EAE and oestrogen receptor β ligand-treated EAE groups (iv). (**B**) Quantification of the number of PLP-EGFP$^+$, olig2$^+$ and GST-pi$^+$ cells per 400 μm^2 indicated a significant decrease in the number of PLP-EGFP$^+$ cells, no change in olig2$^+$ cells and a significant decrease in GST-pi$^+$ cells in vehicle-treated EAE mice compared to normal controls. Oestrogen receptor β ligand treatment caused a significant increase in PLP-EGFP$^+$ cells, no change in olig2$^+$ and a significant increase in GST-pi$^+$ cells compared with vehicle-treated EAE (*$P < 0.05$, ANOVAs; Bonferroni's multiple comparison post test; $n = 8$–10 mice in each treatment group).

GST-pi$^+$ cells than vehicle-treated mice and were similar to normal oligodendrocyte numbers (Fig. 3A and B).

Increased myelin thickness and decreased *g* ratio of callosal axons in oestrogen receptor β ligand-treated experimental autoimmune encephalomyelitis

An increased number of myelinating cells could lead to improved myelination. Therefore, the degree of myelination was first determined by analysing myelin by immunohistochemistry. Myelin basic protein fluorescence intensity measurements indicated significant callosal demyelination of vehicle-treated EAE mice compared to normal (Fig. 4A and B and Supplementary Figs 1 and 2). In contrast, oestrogen receptor β ligand-treated EAE mice had significantly improved myelination that was similar to normal mice (Fig. 4A and B). To assess the integrity of myelination ultrastructure, calculation of axon diameter, myelin thickness and mean *g* ratio of myelinated and unmyelinated axons was performed by electron microscopy analysis (Fig. 5). Vehicle-treated EAE mice at Day 36 of EAE had increased numbers of unmyelinated and thinly myelinated callosal fibres compared to normal

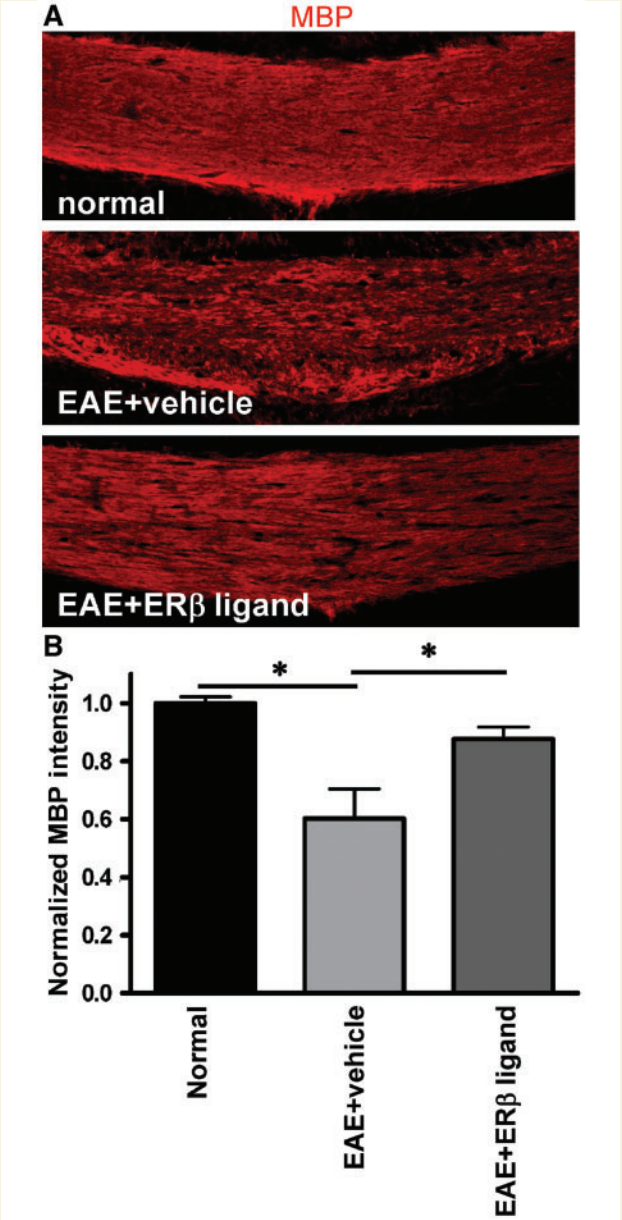

Figure 4 Treatment with an oestrogen receptor β ligand preserved myelin basic protein (MBP) immunoreactivity in the corpus callosum of mice with EAE. (**A**) Brain sections at Day 36 after disease induction were post-fixed, immunostained with anti-myelin basic protein (red) and imaged at ×10 magnification. Vehicle-treated mice had reduced myelin basic protein immunoreactivity as compared to normal controls, while oestrogen receptor β ligand-treated EAE mice showed relatively preserved myelin basic protein staining. (**B**) Upon quantification, myelin basic protein immunoreactivity in the corpus callosum was significantly lower in vehicle-treated EAE mice as compared to normal mice, while oestrogen receptor β ligand-treated EAE mice demonstrated no significant decreases. Myelin intensity is presented as percent of normal (*$P < 0.05$; ANOVAs; Bonferroni's multiple comparison post test; $n = 8$–10 mice in each treatment group).

mice. Activated microglia and astrocytes present in the corpus callosum were accompanied by vacuoles and enlarged mitochondria in axons (Fig. 5A). The corpus callosum of oestrogen receptor β ligand-treated EAE mice appeared to have increased numbers of myelinated fibres as compared to vehicle-treated EAE mice, with the continued presence of activated microglia and some axons with vacuoles and enlarged mitochondria (Fig. 5A). The most dramatic effect of oestrogen receptor β ligand treatment was on the myelin sheath thickness. The callosal axons of oestrogen receptor β ligand-treated EAE mice had significantly thicker myelin than vehicle-treated mice and occasionally thicker myelin than normal mice (Fig. 5A). Even though there were similar demyelinated regions in the perivascular regions due to continued infiltration, nearby axons in oestrogen receptor β ligand-treated mice had thicker myelin compared with axons of vehicle-treated mice (Fig. 5B). Quantitative measurement of myelin sheath thickness of all axons within a given field showed nearly 2-fold increase in oestrogen receptor β ligand-treated EAE mice (0.065 ± 0.002 μm) over vehicle-treated EAE mice (0.027 ± 0.001 μm), and essentially the same thickness as normal mice (0.060 ± 0.002 μm) [Fig. 5C(i)]. Thus, the *g* ratio was significantly lower in the oestrogen receptor β ligand-treated EAE corpus callosum (0.85 ± 0.012), relative to vehicle-treated EAE corpus callosum (0.94 ± 0.026) ($P < 0.05$). The *g* ratio of oestrogen receptor β ligand-treated EAE mice was similar to that of the normal control group [0.87 ± 0.004; Fig. 5C(ii)]. Scatter plots of *g* ratio versus axon diameter highlight the fact that the *g* ratios were higher in the vehicle-treated EAE corpus callosum than in the oestrogen receptor β ligand-treated EAE corpus callosum [Fig. 5C(iii)]. Comparing scatter plots of axon diameter versus *g* ratio or axon diameter versus myelin thickness allowed us to identify the cause of *g*-ratio decrease due to increased myelin thickness in the oestrogen receptor β ligand-treated EAE group. Callosal axons of small to medium sizes showed a more robust increase in myelination with oestrogen receptor β treatment compared with vehicle-treated EAE or normal controls [Fig. 5C(iii) and (iv)].

Oestrogen receptor β ligand treatment reduces experimental autoimmune encephalomyelitis-induced axon damage and limits experimental autoimmune encephalomyelitis-induced disorganization of nodal proteins in callosal axons

Chronic EAE-induced demyelination is accompanied by significant axon damage that could theoretically be reversed by the increased axon myelination observed in oestrogen receptor β ligand-treated EAE mice. Decreased axon damage during EAE was confirmed by performing immunohistochemistry with NF200, a common axon marker, and β-amyloid precursor protein, a marker of axon damage. In normal controls, NF200 was visible in small areas (probably nodes of Ranvier) of myelinated axons that were co-stained with myelin basic protein [Fig. 6A(i)]. Furthermore, there was no significant β-amyloid precursor protein

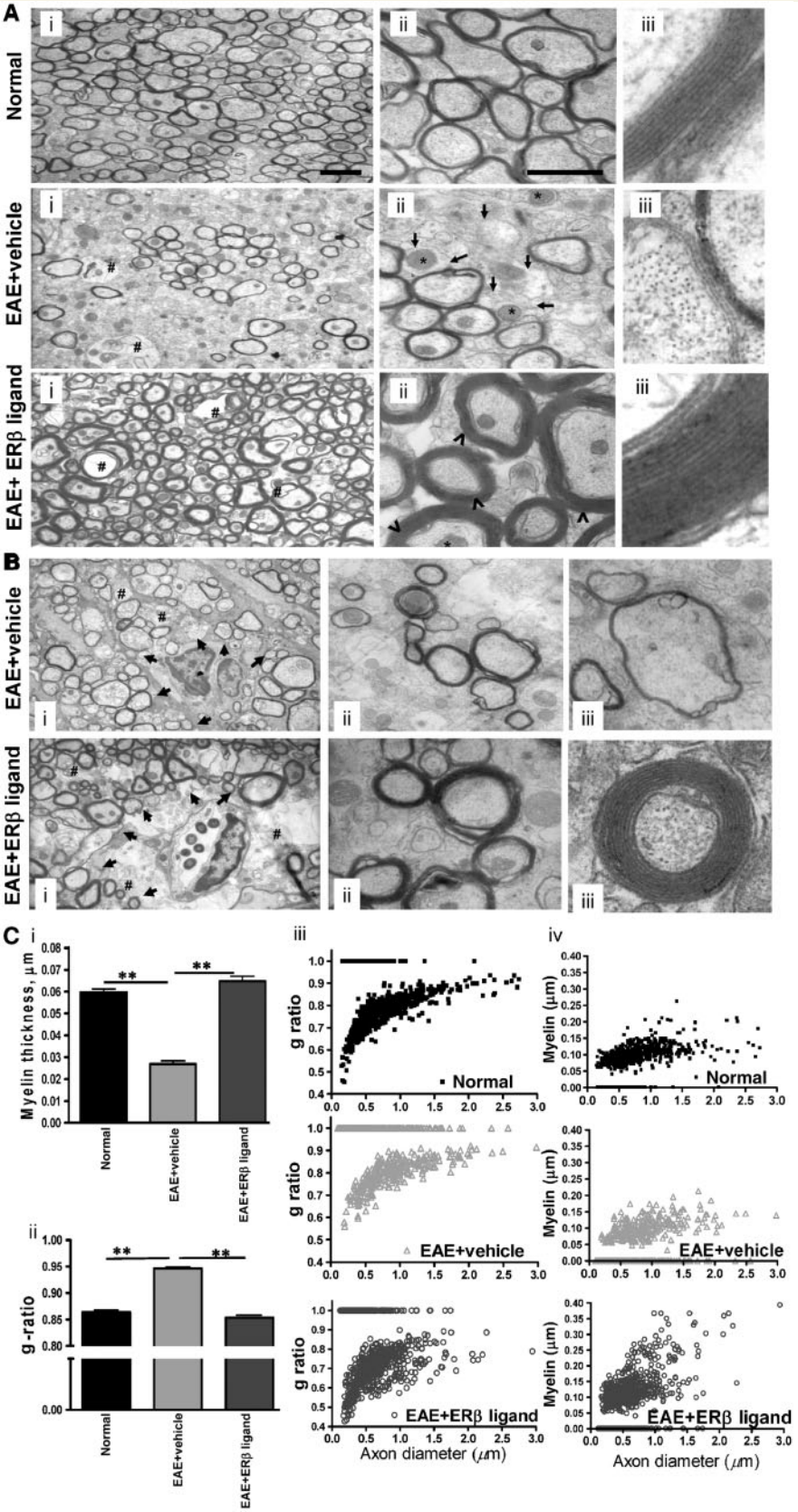

Figure 5 Oestrogen receptor β ligand-treated EAE callosal axons have thicker myelin. (**A**) Representative electron micrographs of the corpus callosum from normal control, vehicle-treated EAE and oestrogen receptor β ligand-treated EAE mice show differential levels of axon myelination [(i)–(iii)]. Compared to normal controls, the corpus callosum of vehicle-treated EAE mice show increased numbers of unmyelinated axons with enlarged mitochondria. Oestrogen receptor β ligand treatment during EAE resulted in a dramatic increase in

Continued

immunoreactivity, thereby indicating intact, healthy axons [Fig. 6B(i) and C]. In contrast, vehicle-treated EAE axons had large areas of NF200 positivity and minimal myelin basic protein staining, denoting demyelination [Fig. 6A(ii)]. In addition, these demyelinated axons showed β-amyloid precursor protein immunoreactive axonal swelling, axon bulbs and transected axons in the corpus callosum white matter [Fig. 6B(ii) and C]. Callosal axons of oestrogen receptor β ligand-treated EAE mice showed less demyelination and a reduced amount of β-amyloid precursor protein immunoreactivity than vehicle-treated EAE mice (Fig. 6).

Saltatory conduction of myelinated axons depends on the presence of nodes of Ranvier on healthy axons (Waxman, 2006). Demyelination leading to nodal disorganization and axon damage is prominent in multiple sclerosis lesions and is probably a major cause of conduction failure. Similar nodal disorganization and conduction failure has been observed in EAE spinal cord (Craner *et al.*, 2004). Therefore, the effect of EAE-induced demyelination and oestrogen receptor β ligand treatment-induced hypermyelination on nodal proteins was analysed in the corpus callosum. Nodal regions were identified and delineated with antibodies against Caspr, a component of axo–glial junctions that appears paranodally. In the corpus callosum of normal mice, Nav1.6$^+$ staining was found mostly between Caspr$^+$ staining, clearly identifying nodes of Ranvier (Fig. 7A). During chronic EAE, Caspr staining levels were decreased significantly to <60% of normal corpus callosum (Fig. 7B). Surprisingly, intact Caspr pairs contained Nav1.6 at the nodes, similar to normal corpus callosum. The remaining Nav1.6 protein, instead of being concentrated between Caspr pairs, had become diffuse over the length of the axons (Fig. 7A), as previously seen in multiple sclerosis and EAE tissue (Craner *et al.*, 2004; Black *et al.*, 2007).

Kv1.2 potassium channel proteins appear as juxtaparanodal pairs in normal myelinated axons (Fig. 7C). Demyelination in vehicle-treated EAE was associated with increased expression of Kv1.2 and a lengthening of Kv1.2 immunostaining across the entire axon length. Oestrogen receptor β ligand-treated EAE callosal axons had only a few areas of diffuse Kv1.2 staining, but overall showed near normal levels of juxtaparanodal Kv1.2 staining (Fig. 7C).

Oestrogen receptor β ligand treatment during experimental autoimmune encephalomyelitis restores callosal conduction, axon velocity and axon refractoriness of callosal axons

Callosal axons play a major role in interhemispheric transfer and integration of sensorimotor and cognitive information (Singer, 1995). To characterize the functional consequences of the neuropathology in the corpus callosum during EAE, compound action potentials were recorded in callosal axons (Fig. 8). Coronal brain slices with midline-crossing segments of the corpus callosum, corresponding approximately to Plates 29–48 in the atlas of Paxinos and Franklin (2001), were used for recording. Two downward phases of the compound action potentials N1 and N2 were observed, probably representing fast depolarization from large, myelinated axons and slower depolarization from non-myelinated axons, respectively (Crawford *et al.*, 2009*a*). Typical voltage traces are shown in Fig. 8B. During early EAE (Day 20), both N1 and N2 compound action potential amplitudes were decreased to ~50% of normal ($P<0.001$, Fig. 8C and D). This decrease persisted later into EAE (Day 36). Treatment with oestrogen receptor β ligand during EAE induced an increase in N1 and N2 compared with vehicle-treated mice, which was a trend when examined early, but became significant when examined late ($P<0.05$, Fig. 8D).

The myelinated compound action potential component N1 of oestrogen receptor β ligand-treated EAE callosal axons showed a small but significant shift to the left of vehicle-treated EAE callosal axons (Fig. 8B). A shift to the left could theoretically be due to an increase in axon conduction velocity as a consequence of improved myelination. To confirm this we first measured conduction velocity of EAE callosal axons in the absence and presence of oestrogen receptor β ligand treatment as previously described (Crawford *et al.*, 2009*a*). The peak latency of the N1 and N2 components were measured and graphed versus distance. Linear regression analysis was performed for each compound action potential component to yield a slope that is the inverse of the velocity, followed by statistical comparison of the velocities. The

Figure 5 Continued
myelination of mostly smaller axons as compared with vehicle-treated EAE and normal control. Pictures are at (i) ×4800; (ii) ×19 000 and (iii) ×48 000 magnification. Scale bar is 1 μm. Arrow = de/un-myelinated axons; ^ = thicker myelin sheath; * = enlarged mitochondria; # = vacuoles. (**B**) Additional examples of vehicle-treated EAE and oestrogen receptor β ligand-treated EAE callosal axons near a lesion with infiltrating cells. Notice that there are areas in the oestrogen receptor β ligand-treated corpus callosum that contain many demyelinating damaged axons similar to those seen extensively in vehicle-treated EAE mice (i). The remaining axons in oestrogen receptor β ligand-treated EAE mice (ii) have thicker myelin sheath compared with vehicle-treated EAE mice (iii). (**C**) Measurement of myelin thickness showed significant decrease in vehicle-treated EAE mice as compared with normal and oestrogen receptor β ligand-treated EAE mice (i). Axon diameter and fibre diameter were measured to further quantify the degree of myelination. Axon diameter/fibre diameter (*g* ratio) showed a significant increase in vehicle-treated callosal axons and a dramatic decrease in *g* ratio was observed in oestrogen receptor β ligand-treated EAE callosal axons (ii). Scatter plots of axon diameter versus *g* ratio (iii) and axon diameter versus myelin thickness (iv) indicated demyelination-induced decreases in myelin thickness in vehicle-treated EAE callosal axons, whereas oestrogen receptor β ligand-treated EAE mice show increased myelination of small–medium-sized callosal axons. The increase in callosal axon *g* ratio of vehicle-treated corpus callosum was due to demyelination of axons, whereas the decrease in *g* ratio in oestrogen receptor β ligand-treated callosal axons was due to an increase in myelination of axons. *$P< 0.05$. ANOVAs; Bonferroni's multiple comparison post test. At least four mice (36 days post EAE induction) from each group were analysed and a minimum of 500 fibres were measured from each mouse.

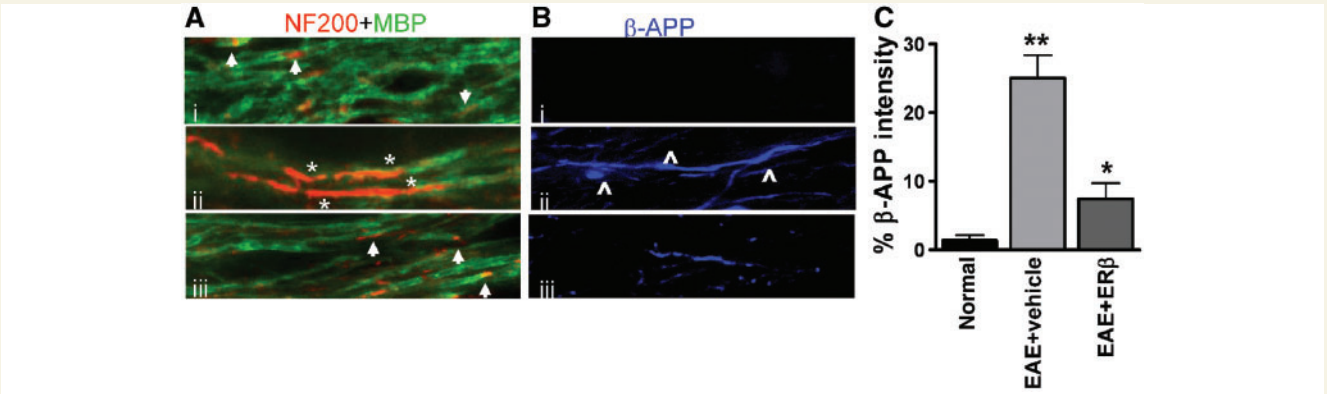

Figure 6 Decrease in demyelination and axon damage in oestrogen receptor β ligand-treated EAE callosal axons. (**A**) High magnification confocal images (×60) were taken to identify the presence of demyelination and axon damage. Normal myelinated axons (i) had even myelin basic protein (MBP) immunostaining with small areas that were MBP^- and $NF200^+$ and are most likely the nodes of Ranvier (arrow). Vehicle-treated EAE axons (ii) expressed large areas that were MBP^- and $NF200^+$ indicative of demyelination (*). Oestrogen receptor β ligand treatment during EAE (iii) had myelinated axons similar to normal. (**B**) Axon degeneration was assessed with β-amyloid precursor protein accumulation. Unlike the normal control corpus callosum that did not show axonal pathology with β-amyloid precursor $protein^-$ immunostaining (blue), vehicle-treated EAE mice had demyelinated axons that showed swelling, beading (^) and increased areas of β-amyloid precursor protein accumulation. Oestrogen receptor β treatment during EAE significantly reduced the extent of axon pathology. (**C**) Quantification of β-amyloid precursor protein immunostaining intensity in the corpus callosum showed nearly 70% less accumulation in oestrogen receptor β ligand-treated EAE compared to vehicle-treated EAE. $*P<0.05$; $**P<0.001$, ANOVAs; Bonferroni's multiple comparison post test; $n=5$ mice in each treatment group.

conduction velocity of the N1 component for normal callosal axons was 1.82 ± 0.15 m/s whereas the N1 conduction velocity of vehicle-treated EAE decreased to 1.69 ± 0.10 m/s. Oestrogen receptor β ligand treatment during EAE induced an increase in conduction velocity to 1.92 ± 0.11 m/s, a significant increase compared with both vehicle-treated EAE and the normal group. The conduction velocity of the N2 component was not different between normal and treatment groups and was 0.57 ± 0.012 (normal), 0.55 ± 0.20 (vehicle-treated EAE) and 0.56 ± 0.10 (oestrogen receptor β ligand-treated EAE) m/s. In conclusion, oestrogen receptor β ligand-treated EAE callosal axons showed a slight but significant improvement in conduction velocity.

Chronic EAE-induced demyelination and conduction deficit is also accompanied by functional axon deficit. Axonal deficits were estimated by assaying changes in axon refractoriness as previously described (Reeves *et al.*, 2005; Crawford *et al.*, 2009*a*). Figure 9A shows an example series of the second response evoked in paired stimulus presentations, after subtracting out the response to a conditioning pulse. Traces shown are for normal, vehicle-treated EAE and oestrogen receptor β ligand-treated EAE mice at interpulse intervals from 2–8 ms. The compound action potential component-amplitude elicited by the second pulse in each paired stimulation (C_2) divided by the compound action potential component-amplitude to single pulse stimulation (C_1) was plotted. These C_2/C_1 ratios were averaged for each analytical group and mean values fitted to Boltzmann sigmoid curves. Rightward shifts in these curves correspond to increases in the refractory recovery cycle in the callosal axons and are indicative of functional axonal deficit (Reeves *et al.*, 2005; Crawford *et al.*, 2009*a*).

In the normal group, the N1 component evoked by the second of a pair of pulses was 50% of the amplitude of a single pulse presentation when the interpulse interval was 2.2 ± 0.21 ms. The interpulse interval for vehicle-treated EAE had slower responses of 3.9 ± 0.15 ms. Oestrogen receptor β ligand-treated callosal EAE axons had an interpulse interval of 3.0 ± 0.11 ms (Fig. 9B), significantly better than the interpulse interval of vehicle-treated EAE callosal axons. The interpulse intervals for the N2 component of all three groups were not significantly different at 3.1 ± 0.10 ms (normal), 3.5 ± 0.05 ms (vehicle-treated EAE) and 3.1 ± 0.16 ms (oestrogen receptor β ligand-treated EAE).

Callosal and corticospinal tracts are preserved during oestrogen receptor β ligand treatment

Finally, to assess the extent of EAE-induced axon degeneration and the effects of oestrogen receptor β ligand treatment during EAE; the callosal tracts were evaluated by neuronal tract tracing studies. Using a precise micro-injector, each group of mice was injected with the tract dye, dextran red (molecular weight of 10 000) in the right hemisphere. The injection site was the primary motor and sensorimotor cortex near layers II–V to label the pyramidal neurons, thereby establishing a direct labelling method to evaluate these axon tracts.

Previous studies have shown a disruption of DiI–dye-labelled corticospinal axonal damage in spinal cord of EAE mice (Liu *et al.*, 2008). We confirmed our method of labelling by first analysing the EAE corticospinal tract. In the rodent, the only neurons in the forebrain that send axons to the spinal cord are those of the corticospinal tract through the internal capsule and medullary pyramid. Most of the corticospinal tract decussates to the opposite

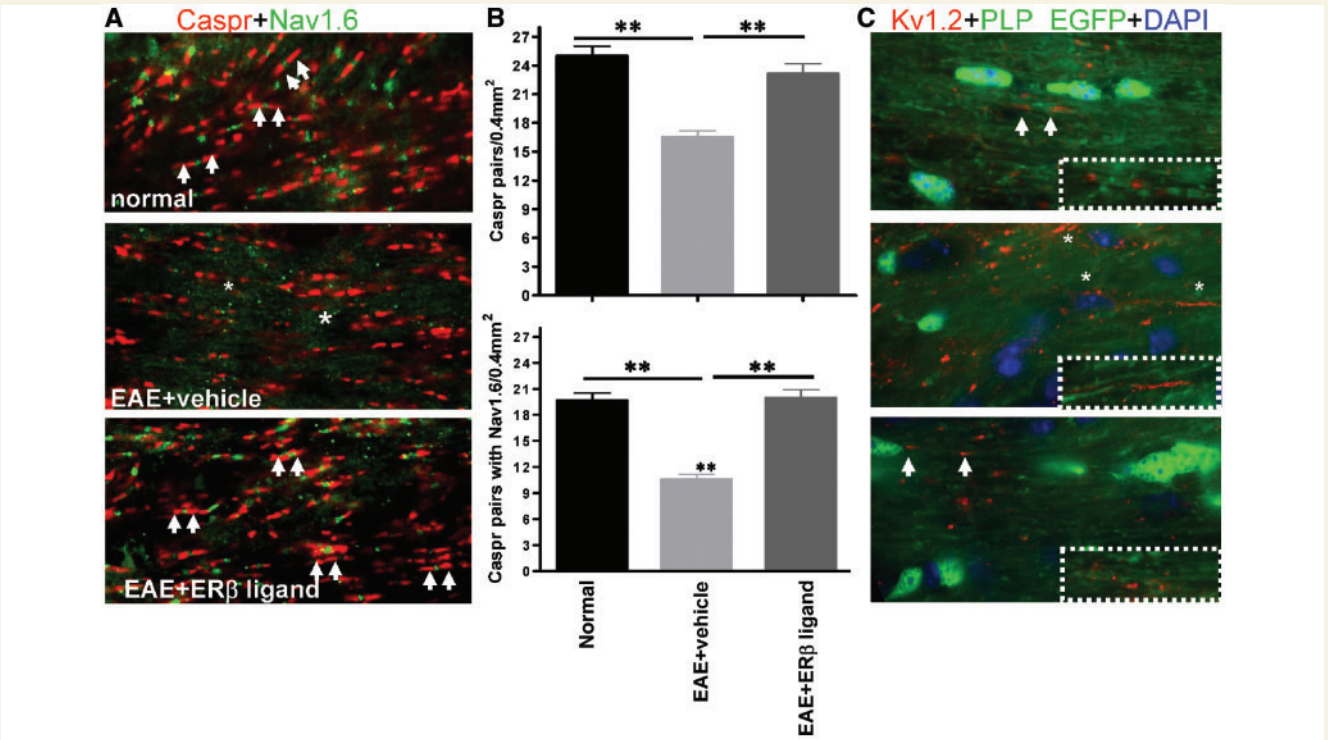

Figure 7 Oestrogen receptor β ligand treatment limits EAE-induced disorganization of nodal proteins in callosal axons. (**A**) Corpus callosum sections were immunostained with nodal proteins Caspr (red, marked with white arrows) and Nav1.6 (green). A significant decrease in Caspr and Nav1.6 staining occurred in the corpus callosum of vehicle-treated EAE mice. In addition, extensive regions of axons (*) were immunostained with Nav1.6 not confined between Caspr pairs. Oestrogen receptor β ligand-treated EAE corpus callosum axons contained Caspr pairs with Nav1.6 similar to normal control. Note: PLP-EGFP-green channel was dropped and Nav1.6 immunostaining performed with TRITC conjugated secondary was pseudo-coloured to green for clarity. (**B**) Quantification of Caspr protein pairs alone and Caspr protein pair encompassing Nav1.6 protein showed a significant decrease in vehicle-treated EAE callosal axons compared to those of normal and oestrogen receptor β ligand-treated EAE. $^{**}P<0.001$, ANOVAs; Bonferroni's multiple comparison post test; $n=5$ mice in each treatment group. (**C**) Juxtaparanodal Kv1.2 protein (red, arrows) immunostaining increased in the corpus callosum of vehicle-treated EAE mice. Specifically, Kv1.2 immunostaining was obvious throughout the length of some axons (*). No significant difference was observed in oestrogen receptor β ligand-treated EAE axons compared with normal.

side in the medulla oblongata and descends in the most ventral part of spinal dorsal funiculus. Unilateral labelling of the corticospinal tract located in the internal capsule, medullary pyramids and at the ventral aspect of the cervical dorsal columns in the cord was clearly visible in normal mice. These regions were labelled discretely by dextran red fluorescence and their individual axons were identifiable (Fig. 10A). However, compared to normal controls, vehicle-treated EAE mice had reduced and discontinuous tract dye staining, indicating dysfunction in the corticospinal tract. The oestrogen receptor β ligand-treated EAE group had significantly improved dye staining compared with vehicle-treated EAE mice (Fig. 10A). Very few dye-filled discontinuous and swollen axon varicosities were present in the oestrogen receptor β ligand-treated animals. Quantification of dextran red dye or $NF200^{+}$ axon intensity showed a significant decrease in the dorsal column during vehicle treatment, whereas oestrogen receptor β ligand treatment showed similar staining to the normal group (Fig. 10B).

Dextran red-labelled axons from layer II/III and layer V descend and cross in the corpus callosum (Fig. 10C). In normal controls, bundles of axons that started from the right side of corpus callosum were labelled with dextran red and crossed over to the left hemisphere. Comparatively, fewer labelled axons crossed over to the left hemisphere in the vehicle-treated EAE mice. Here, the dye fluorescence was punctate and discontinuous, indicative of axon transport deficits. In contrast, oestrogen receptor β ligand-treated EAE mice showed much better labelling compared with vehicle-treated EAE. Nearly 80% of callosal axons in oestrogen receptor β ligand-treated EAE animals were labelled and very few axons showed punctate dye accumulation (Fig. 10C and D).

Discussion

In multiple sclerosis and EAE, although resident oligodendrocyte progenitors are found around the lesions, they remain in a quiescent state (Prineas and Connell, 1979; Reynolds *et al.*, 2001; Back *et al.*, 2005). This differentiation block of oligodendrocyte progenitors contributes to failed remyelination (Franklin and ffrench-

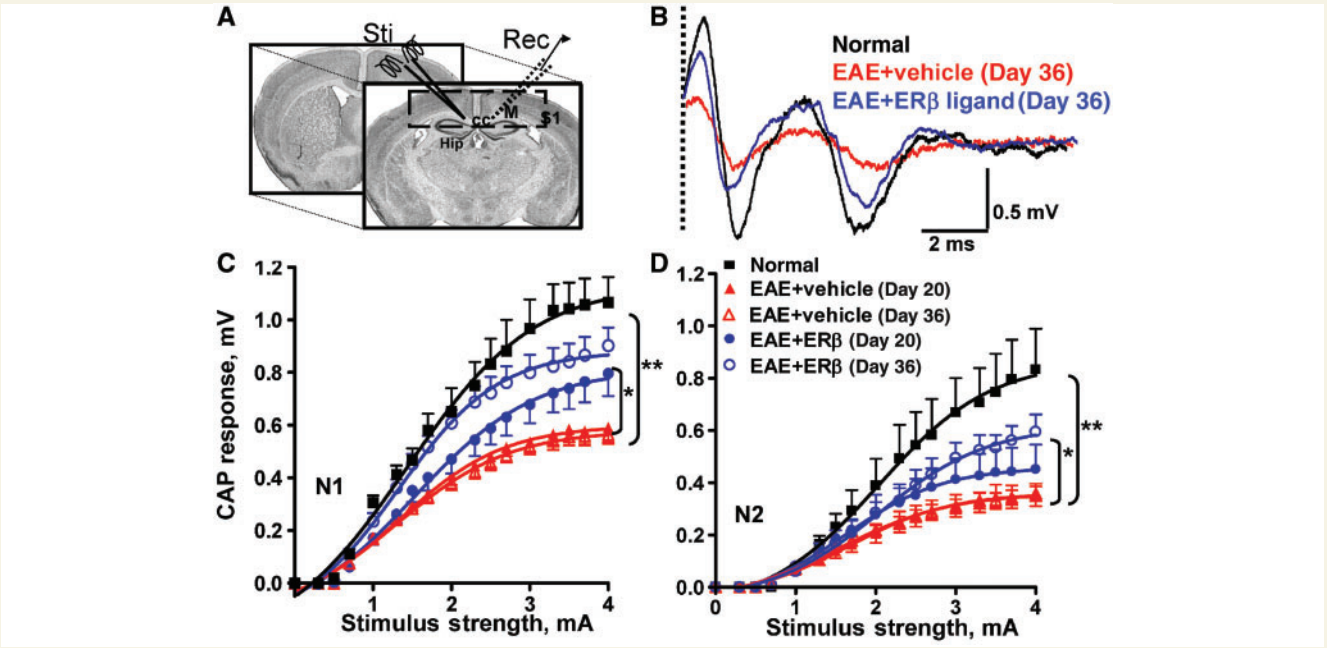

Figure 8 Treatment with oestrogen receptor β ligand restores callosal conduction of both myelinated and non-myelinated axons of mice with EAE. (**A**) Compound action potential (CAP) responses were recorded from slices with midline-crossing segments of the corpus callosum overlying the mid-dorsal hippocampus. Stimulating (Sti) and recording (Rec) electrodes were each placed ~1 mm away from midline. (**B**) Typical corpus callosum compound action potentials from normal (black), vehicle-treated EAE (red) and oestrogen receptor β ligand-treated EAE (blue) brain slices evoked (at a stimulus of 4 mA) at Day 36 after disease induction. There is a decrease in N1 and N2 amplitude in the vehicle-treated EAE group. Treatment with oestrogen receptor β ligand during EAE induced a latency shift in N1 peak, as well as a muted decrease in N1 and N2 compound action potential amplitude compared with vehicle alone (dashed vertical line represents compound action potentials beyond the stimulus artefact). (**C** and **D**) Quantification of N1 and N2 compound action potential amplitudes in the corpus callosum of vehicle-treated EAE mice showed a significant decrease early, at Day 20, and late, at Day 36, after disease induction. Oestrogen receptor β ligand treatment showed a significant improvement in compound action potential response late in disease. Number of mice = 4 per treatment group, number of corpus callosum sections per mouse = 3, total number of sections per treatment group = 12. Statistically significant compared with normal at 2–4 mA stimulus strength. $*P < 0.05$, $**P < 0.001$; ANOVAs; Bonferroni's multiple comparison post test; CC = corpus callosum; Hip = hippocampus; M = motor cortex; S1 = somatosensory cortex.

Constant, 2008; Kuhlmann *et al.*, 2008). The inefficiency or failure of myelin-forming oligodendrocytes to remyelinate axons and preserve axonal integrity remains a major impediment in the repair of multiple sclerosis lesions and is principally responsible for axonal and neuronal degeneration leading to chronic disability (Pagani *et al.*, 2005; Trapp and Nave, 2008).

The adult nervous system maintains a pool of undifferentiated oligodendrocyte progenitors that can migrate to demyelinated axons, differentiate to mature oligodendrocytes and remyelinate axons. Remyelination occurs in many multiple sclerosis lesions early in the disease (Kornek *et al.*, 2000; Patrikios *et al.*, 2006). Unfortunately, cycles of demyelination apparently exhaust the capacity for tissue repair and remyelination eventually becomes less successful (Linington *et al.*, 1992; Patrikios *et al.*, 2006). Myelin regeneration can be improved either by cell replacement therapy, as a substitute to the endogenous pool of oligodendrocyte progenitors, or by boosting the brain's intrinsic capacity for remyelination. The development of neuroprotective treatments that prevent the loss of progenitors and promote the proliferation and differentiation of this cell population are theoretical treatment goals for multiple sclerosis.

The role of oestrogen and oestrogen receptor ligands as neuroprotective agents in EAE, and recently multiple sclerosis, has been extensively investigated by our group (Kim *et al.*, 1999; Morales *et al.*, 2006; Tiwari-Woodruff *et al.*, 2007; Gold *et al.*, 2009). Evidence suggests that oestrogen receptor β ligand treatment before active EAE induction is directly neuroprotective since it preserved spinal cord myelin and prevented axonal loss without reducing CNS inflammation (Tiwari-Woodruff *et al.*, 2007). The neuroprotective effects of the oestrogen receptor β ligand are not mutually exclusive with other effects of treatment on CNS inflammatory cells that may not be detectable by assessing levels of CNS inflammation. One would have to isolate macrophages from EAE lesions in both treated and untreated CNS and analyse their function. Notably, in previous studies, we found that oestrogen receptor β ligand of active EAE was neuroprotective without altering cytokine production in peripheral immune cells (Tiwari-Woodruff *et al.*, 2007).

Efficacy of oestrogen treatments during EAE or multiple sclerosis will probably depend on its early administration, before significant CNS damage has occurred (Brinton, 2005). Oestrogen receptor β ligand treatment before active EAE induction allowed us to

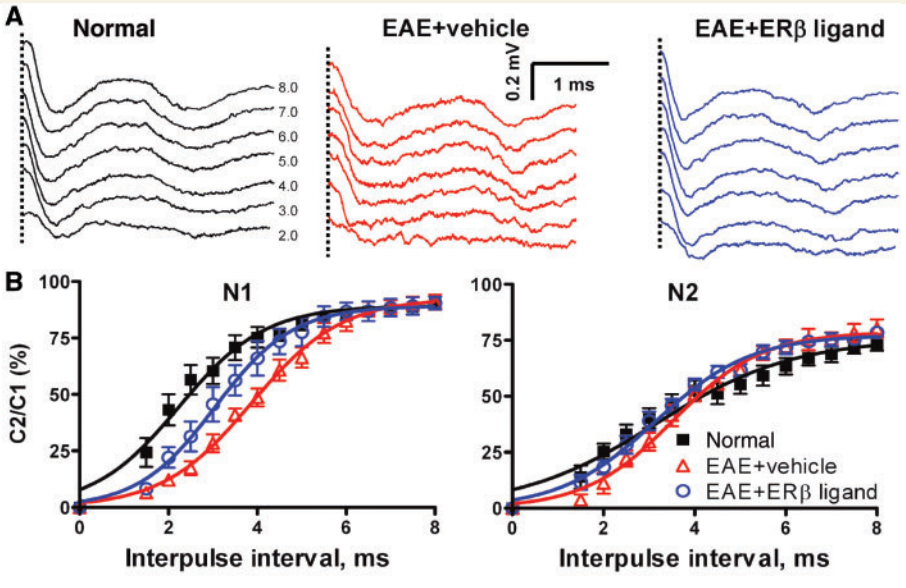

Group	N1 (ms)	N2 (ms)
Normal	2.2 ± 0.21	3.1 ± 0.12
EAE+vehicle	3.9 ± 0.15	3.5 ± 0.20
EAE+ERβ ligand	3.0 ± 0.11	3.1 ± 0.22

Figure 9 Treatment with oestrogen receptor β ligand restores refractoriness of callosal axons. (**A**) Example waveforms shows the second response in paired stimuli after subtraction of the response to the conditioning pulse (interpulse intervals = 2–8 ms) for normal, vehicle-treated EAE and oestrogen receptor β ligand-treated EAE callosal axons at later time point (dashed vertical line represents compound action potentials beyond the stimulus artefact). (**B**) Average C_2/C_1 ratios [obtained from plots of mean compound action potential amplitude elicited by the second pulse in each paired stimulation (C_2) divided by the compound action potential amplitude to single pulse stimulation (C_1)] were fitted to Boltzmann sigmoid curves. A rightward shift in curves for N1 shows decreased refractoriness in vehicle-treated and oestrogen receptor β ligand-treated EAE groups ($n = 4$). Oestrogen receptor β ligand-treated EAE callosal axons show a significant increase (a leftward shift in the curve compared with vehicle treatment alone) in refractoriness of N1 compared with those with vehicle treatment alone. The interpulse interval values (mean ± SD) of N1 and N2 component for normal, vehicle-treated EAE and oestrogen receptor β ligand-treated EAE callosal axons are presented in the table.

investigate the potential for oestrogens to prevent against damage mediated by the first inflammatory attack. In established relapsing–remitting multiple sclerosis, this may simulate protection from damage during the next relapse. Notably, once the oestrogen therapy-induced neuroprotective targets have been established, we will, in future studies, assess the critical period of oestrogen treatment at various timepoints during disease.

In the present study, we used a combination of electrophysiological field potentials, electron microscopy, tract tracing and immunohistochemical analyses to address whether oestrogen receptor β ligand treatment might provide functional recovery. Functional recovery of axons during treatments of multiple sclerosis models has not been previously addressed using such a combination of complementary modalities. We focused primarily in the corpus callosum since it is commonly targeted in multiple sclerosis and is amenable to repair by the above modalities (Ozturk *et al.*, 2001; Pelletier *et al.*, 2001).

Oestrogen receptor β ligand treatment increased the number of myelinating oligodendrocytes and stimulated axon myelination in the corpus callosum. This increase in myelination with oestrogen receptor β ligand treatment during EAE was functionally relevant as it led to improved axon conduction and decreased axon deficit. Oestrogen receptor β ligand treatment was not mediated by an effect on inflammation, as no significant differences in immune cells and astrocytes between vehicle-treated and oestrogen receptor β ligand-treated EAE mice were observed. A more direct effect of oestrogens on oligodendrocytes is likely since oestrogen receptors (α and β) are present on oligodendrocyte lineage cells (Takao *et al.*, 2004; Zhang *et al.*, 2004). In addition, oestrogens that bind oestrogen receptor α and oestrogen receptor β, notably oestradiol, have various effects on oligodendrocyte functions including delaying the exit of oligodendrocyte progenitors from the cell cycle, enhancing myelin membrane sheath formation (Marin-Husstege *et al.*, 2004) and enhancing oligodendrocyte synthesis of myelin basic protein in primary oligodendrocyte cultures. Oestradiol also promotes remyelination in dorsal root ganglion and Schwann cell co-cultures (Zhu and Glaser, 2008), cuprizone demyelination and ischaemia mouse models (Gerstner *et al.*, 2007; Kipp and Beyer, 2009).

Crosstalk between oestrogen receptor β and other growth factor receptors such as insulin-like growth factor-1 could be

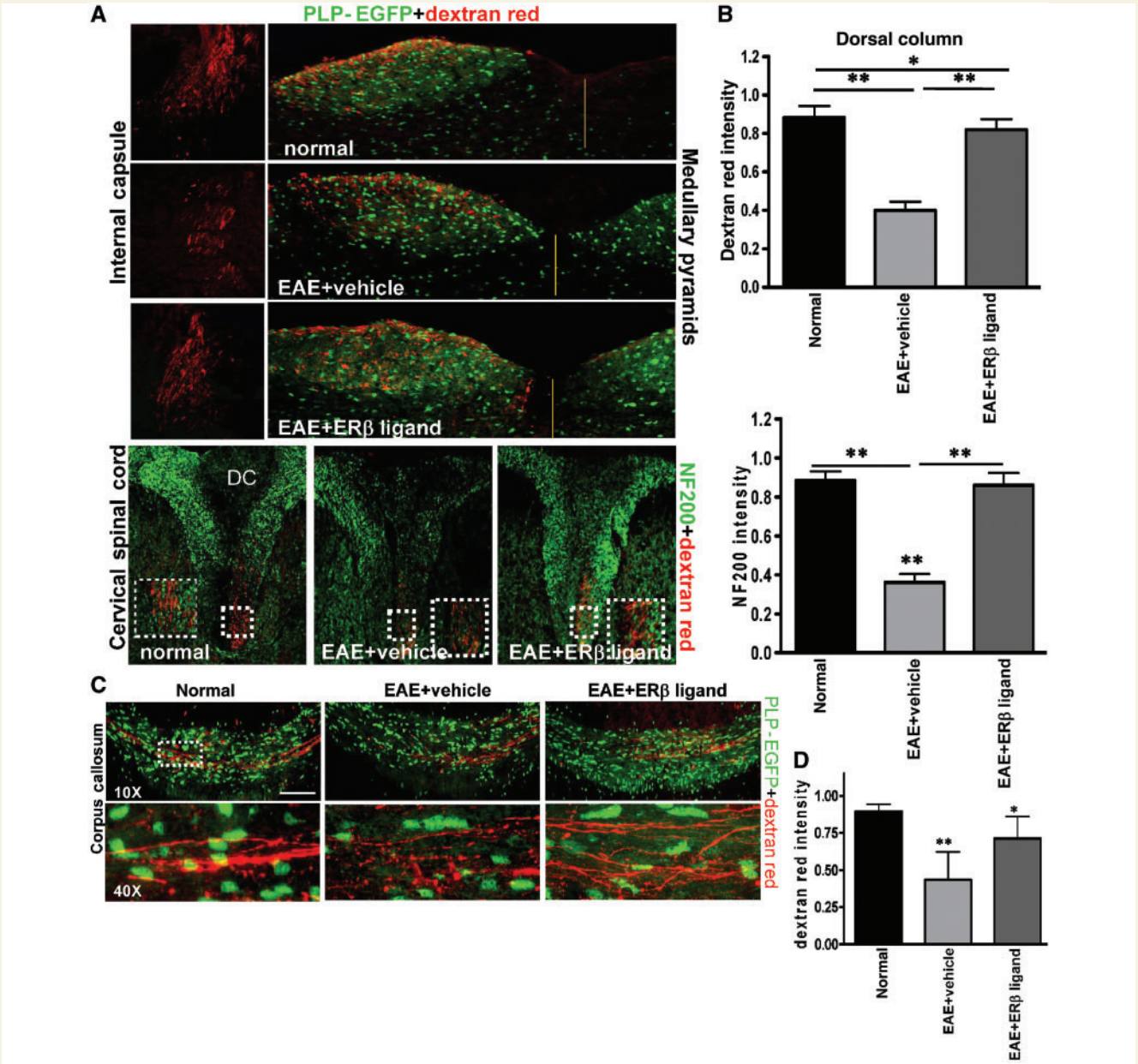

Figure 10 Oestrogen receptor β ligand treatment prevented corticospinal tract and callosal pathology induced by EAE. (**A**) The corticospinal tract from layer II/III and layer V neurons were followed through the internal capsule (dextran red only), medullary pyramids (dextran red and PLP-EGFP) and the spinal cord (dextran red and NF200) in the ventral-most part of the dorsal column (DC). Dextran red labelling was decreased in these areas in the vehicle-treated EAE compared to those of normal. Oestrogen receptor β ligand-treated EAE showed improvement, especially in the high cervical spinal cord. Fluorescent red axons were seen only in one side and the axon intensity was measured from single confocal images of high cervical spinal cord. At the cervical level, the dextran labelled axon number of vehicle-treated EAE mice was significantly decreased compared to normal mice, while the oestrogen receptor β ligand-treated EAE axons showed increased numbers similar to normal controls. (**B**) Cervical spinal cord sections from normal, vehicle-treated and oestrogen receptor β ligand-treated EAE animals that were injected with dextran red were co-immunostained with NF200 (green). Dorsal column was delineated and dextran red and NF200 fluorescence intensity were calculated and normalized to normal. Vehicle-treated EAE dorsal column showed a significant decrease in dextran red and NF200 fluorescence, whereas oestrogen receptor β ligand-treated EAE dorsal column had similar levels to normal. $*P<0.05$; $**P<0.001$, ANOVAs; Bonferroni's multiple comparison post test; $n=5$. (**C**) Representative fluorescent images show callosal tracts of normal, vehicle-treated EAE and oestrogen receptor β ligand-treated EAE mice 7 days post-dextran red injection. Normal corpus callosum shows green PLP-EGFP$^+$ cells and intense, coherent dextran red labelling of callosal axons. The corpus callosum of vehicle-treated EAE mice had decreased PLP-EGFP$^+$ cells, as well as decreased, punctate and discontinuous dextran red labelling. Oestrogen receptor β ligand-treated EAE had many more PLP-EGFP$^+$ cells and an increased number of axons that were dextran red labelled compared with vehicle-treated EAE animals. Scale bar is 100 μm. (**D**) Quantification of dextran red intensity in known corpus callosum regions indicated a significant decrease during vehicle-treated EAE compared to normal. Oestrogen receptor β ligand-treated EAE mice were not significantly different than normal control. $*P<0.05$; $**P<0.001$, ANOVAs; Bonferroni's multiple comparison post test; $n=4$.

involved in oligodendrocyte differentiation and survival leading to improved myelination after oestrogen receptor β ligand treatment. Insulin-like growth factor-1, through its binding to the insulin-like growth factor-1 receptor, is known to play a vital role in oligodendrocyte development, survival and myelination (McMorris *et al.*, 1986). Oestradiol is known to induce an increase in insulin-like growth factor-1 during cuprizone demyelination (Acs *et al.*, 2009). Further, the insulin-like growth factor-1 receptor promotes sustained phosphorylation of serine/threonine-specific protein kinases (Akt), which is required for the survival of oligodendrocyte progenitors (Pang *et al.*, 2007; Romanelli *et al.*, 2009). Constitutive activation of Akt leads to the activation of mammalian target of rapamycin, required for oligodendrocyte differentiation and myelination (Narayanan *et al.*, 2009; Tyler *et al.*, 2009). Thus, oestrogen receptor β ligand treatment during EAE may induce a significant increase in the myelination of axons by activating the Akt pathway and mammalian target of rapamycin directly.

The rationale for almost all therapies for multiple sclerosis has been to reduce inflammation. Immunomodulatory therapies, such as interferon-β, glatiramer acetate and mitoxantrone have considerably improved the therapeutic options for patients with multiple sclerosis. These agents reduce relapse rates and reduce appearance of MRI enhancing lesions. However, their efficacy in preventing accumulation of disability and their impact on disease progression has been disappointing (Trojano *et al.*, 2006; Van der Walt *et al.*, 2010). Identifying a drug that stimulates endogenous myelination and spares axon degeneration would theoretically reduce the rate of disease progression.

A few agents such as thyroid hormone (triiodothyronine-T3), leukaemia inhibitory factor and progesterone have shown limited promise. Triiodothyronine-T3 administration during EAE showed no clinical improvement but a small improvement in oligodendrocyte progenitor number and myelin basic protein intensity (Calza *et al.*, 2002; Fernandez *et al.*, 2004). Triiodothyronine-T3 therapy during the remyelination phase after chronic cuprizone demyelination resulted in improved remyelination and an increase in oligodendrocyte progenitors (Franco *et al.*, 2008; Harsan *et al.*, 2008). Leukaemia inhibitory factor, a neuronal survival factor with limited ability to cross the blood–brain barrier and pleiotropic actions outside the CNS, when administered exogenously during EAE, resulted in a small decrease in clinical scores and decreased oligodendrocyte death (Butzkueven *et al.*, 2002; Slaets *et al.*, 2010). In a more recent study, leukaemia inhibitory factor administration decreased cuprizone demyelination, but was unable to show any improvement during remyelination (Emery *et al.*, 2006). Progesterone therapy moderately delayed disease onset, reduced the clinical scores, reduced inflammatory response and reduced the occurrence of demyelination in EAE spinal cord (Garay *et al.*, 2007), but had no effect in the cuprizone model (Acs *et al.*, 2009). None of these studies emphasized the effect of therapy-induced myelination/remyelination on axon conduction and transport such as those observed with oestrogen receptor β ligand treatment. To our knowledge, oestrogen receptor β ligand is the first compound that stimulates myelination and improves axon conduction *in vivo* in the presence of inflammation. The ligand has no known toxicity or blood–brain barrier permeability issues. These observations are of significant clinical relevance, since oestrogen receptor β ligand treatment would probably be very well tolerated as both breast and uterine endometrial cancer are mediated through oestrogen receptor α, not oestrogen receptor β (Rossouw and Harlan, 1994; Beral, 2003). In addition, a neuroprotective agent that enhances myelination such as oestrogen receptor β ligand could be taken in combination with the currently available anti-inflammatory agents. Collectively, this represents a major advance for not only multiple sclerosis, but also other neurodegenerative diseases characterized by a demyelinating component.

Acknowledgements

Our sincere thanks to Ms Umeda for help with EAE induction, Dr Lopez-Valdes for help with electrophysiology setup and Ms Thompson for EM help.

Funding

This work was generously supported by LNE Training Award 5T32HD007228 and NMSS Centre Grant CA1028.

Supplementary material

Supplementary material is available at *Brain* online.

References

Randomised double-blind placebo-controlled study of interferon beta-1a in relapsing/remitting multiple sclerosis. PRISMS (Prevention of Relapses and Disability by Interferon beta-1a Subcutaneously in Multiple Sclerosis) Study Group. Lancet 1998; 352: 1498–504.

Acs P, Kipp M, Norkute A, Johann S, Clarner T, Braun A, et al. 17beta-estradiol and progesterone prevent cuprizone provoked demyelination of corpus callosum in male mice. Glia 2009; 57: 807–14.

Back SA, Tuohy TM, Chen H, Wallingford N, Craig A, Struve J, et al. Hyaluronan accumulates in demyelinated lesions and inhibits oligodendrocyte progenitor maturation. Nat Med 2005; 11: 966–72.

Bannerman PG, Hahn A, Ramirez S, Morley M, Bonnemann C, Yu S, et al. Motor neuron pathology in experimental autoimmune encephalomyelitis: studies in THY1-YFP transgenic mice. Brain 2005; 128: 1877–86.

Beral V. Breast cancer and hormone-replacement therapy in the Million Women Study. Lancet 2003; 362: 419–27.

Black JA, Newcombe J, Trapp BD, Waxman SG. Sodium channel expression within chronic multiple sclerosis plaques. J Neuropathol Exp Neurol 2007; 66: 828–37.

Bonzano L, Tacchino A, Roccatagliata L, Abbruzzese G, Mancardi GL, Bove M. Callosal contributions to simultaneous bimanual finger movements. J Neurosci 2008; 28: 3227–33.

Boroojerdi B, Hungs M, Mull M, Topper R, Noth J. Interhemispheric inhibition in patients with multiple sclerosis. Electroencephalogr Clin Neurophysiol 1998; 109: 230–7.

Brinton RD. Investigative models for determining hormone therapy-induced outcomes in brain: evidence in support of a healthy cell bias of oestrogen action. Ann N Y Acad Sci 2005; 1052: 57–74.

Brown DA, Sawchenko PE. Time course and distribution of inflammatory and neurodegenerative events suggest structural bases for the pathogenesis of experimental autoimmune encephalomyelitis. J Comp Neurol 2007; 502: 236–60.

Butzkueven H, Zhang JG, Soilu-Hanninen M, Hochrein H, Chionh F, Shipham KA, et al. LIF receptor signaling limits immune-mediated demyelination by enhancing oligodendrocyte survival. Nat Med 2002; 8: 613–19.

Calza L, Fernandez M, Giuliani A, Aloe L, Giardino L. Thyroid hormone activates oligodendrocyte precursors and increases a myelin-forming protein and NGF content in the spinal cord during experimental allergic encephalomyelitis. Proc Natl Acad Sci USA 2002; 99: 3258–63.

Carswell HV, Macrae IM, Gallagher L, Harrop E, Horsburgh KJ. Neuroprotection by a selective oestrogen receptor beta agonist in a mouse model of global ischemia. Am J Physiol Heart Circ Physiol 2004; 287: H1501–4.

Chang A, Tourtellotte WW, Rudick R, Trapp BD. Premyelinating oligodendrocytes in chronic lesions of multiple sclerosis. N Engl J Med 2002; 346: 165–73.

Chaovipoch P, Jelks KA, Gerhold LM, West EJ, Chongthammakun S, Floyd CL. 17beta-estradiol is protective in spinal cord injury in post- and pre-menopausal rats. J Neurotrauma 2006; 23: 830–52.

Craner MJ, Hains BC, Lo AC, Black JA, Waxman SG. Co-localization of sodium channel Nav1.6 and the sodium-calcium exchanger at sites of axonal injury in the spinal cord in EAE. Brain 2004; 127: 294–303.

Crawford DK, Mangiardi M, Tiwari-Woodruff SK. Assaying the functional effects of demyelination and remyelination: revisiting field potential recordings. J Neurosci Methods 2009a; 182: 25–33.

Crawford DK, Mangiardi M, Xia X, Lopez-Valdes HE, Tiwari-Woodruff SK. Functional recovery of callosal axons following demyelination: a critical window. Neuroscience 2009b; 164: 1407–21.

Du S, Sandoval F, Trinh P, Voskuhl RR. Additive effects of combination treatment with anti-inflammatory and neuroprotective agents in experimental autoimmune encephalomyelitis. J Neuroimmunol 219: 64–74.

Dubal DB, Rau SW, Shughrue PJ, Zhu H, Yu J, Cashion AB, et al. Differential modulation of oestrogen receptors (ERs) in ischemic brain injury: a role for ERalpha in estradiol-mediated protection against delayed cell death. Endocrinology 2006; 147: 3076–84.

Emery B, Cate HS, Marriott M, Merson T, Binder MD, Snell C, et al. Suppressor of cytokine signaling 3 limits protection of leukemia inhibitory factor receptor signaling against central demyelination. Proc Natl Acad Sci USA 2006; 103: 7859–64.

Fernandez M, Giuliani A, Pirondi S, D'Intino G, Giardino L, Aloe L, et al. Thyroid hormone administration enhances remyelination in chronic demyelinating inflammatory disease. Proc Natl Acad Sci USA 2004; 101: 16363–8.

Filippi M, Rocca MA, Falini A, Caputo D, Ghezzi A, Colombo B, et al. Correlations between structural CNS damage and functional MRI changes in primary progressive MS. Neuroimage 2002; 15: 537–46.

Franco PG, Silvestroff L, Soto EF, Pasquini JM. Thyroid hormones promote differentiation of oligodendrocyte progenitor cells and improve remyelination after cuprizone-induced demyelination. Exp Neurol 2008; 21: 458–67.

Franklin K, Paxinos G. The mouse brain: in stereotaxic coordinates. San Diego: Academic Press; 2001.

Franklin RJ, Ffrench-Constant C. Remyelination in the CNS: from biology to therapy. Nat Rev Neurosci 2008; 9: 839–55.

Frischer JM, Bramow S, Dal-Bianco A, Lucchinetti CF, Rauschka H, Schmidbauer M, et al. The relation between inflammation and neurodegeneration in multiple sclerosis brains. Brain 2009; 132: 1175–89.

Fuss B, Afshari FS, Colello RJ, Macklin WB. Normal CNS myelination in transgenic mice overexpressing MHC class I H-2L(d) in oligodendrocytes. Mol Cell Neurosci 2001; 18: 221–34.

Garay L, Deniselle MC, Lima A, Roig P, De Nicola AF. Effects of progesterone in the spinal cord of a mouse model of multiple sclerosis. J Steroid Biochem Mol Biol 2007; 107: 228–37.

Gasperini C, Ruggieri S. New oral drugs for multiple sclerosis. Neurol Sci 2009; 30 (Suppl 2): S179–83.

Gerstner B, Sifringer M, Dzietko M, Schuller A, Lee J, Simons S, et al. Estradiol attenuates hyperoxia-induced cell death in the developing white matter. Ann Neurol 2007; 61: 562–73.

Gold SM, Sasidhar MV, Morales LB, Du S, Sicotte NL, Tiwari-Woodruff SK, et al. Oestrogen treatment decreases matrix metalloproteinase (MMP)-9 in autoimmune demyelinating disease through oestrogen receptor alpha (ERalpha). Lab Invest 2009; 89: 1076–83.

Groeneveld GJ, van Muiswinkel FL, Sturkenboom JM, Wokke JH, Bar PR, van den Berg LH. Ovariectomy and 17beta-estradiol modulate disease progression of a mouse model of ALS. Brain Res 2004; 1021: 128–31.

Harsan LA, Steibel J, Zaremba A, Agin A, Sapin R, Poulet P, et al. Recovery from chronic demyelination by thyroid hormone therapy: myelinogenesis induction and assessment by diffusion tensor magnetic resonance imaging. J Neurosci 2008; 28: 14189–201.

Hobom M, Storch MK, Weissert R, Maier K, Radhakrishnan A, Kramer B, et al. Mechanisms and time course of neuronal degeneration in experimental autoimmune encephalomyelitis. Brain Pathol 2004; 14: 148–57.

Jones MV, Nguyen TT, Deboy CA, Griffin JW, Whartenby KA, Kerr DA, et al. Behavioral and pathological outcomes in MOG 35-55 experimental autoimmune encephalomyelitis. J Neuroimmunol 2008; 199: 83–93.

Kim S, Liva SM, Dalal MA, Verity MA, Voskuhl RR. Estriol ameliorates autoimmune demyelinating disease: implications for multiple sclerosis. Neurology 1999; 52: 1230–8.

Kipp M, Beyer C. Impact of sex steroids on neuroinflammatory processes and experimental multiple sclerosis. Front Neuroendocrinol 2009; 30: 188–200.

Kornek B, Storch MK, Weissert R, Wallstroem E, Stefferl A, Olsson T, et al. Multiple sclerosis and chronic autoimmune encephalomyelitis: a comparative quantitative study of axonal injury in active, inactive, and remyelinated lesions. Am J Pathol 2000; 157: 267–76.

Kuhlmann T, Miron V, Cui Q, Wegner C, Antel J, Bruck W. Differentiation block of oligodendroglial progenitor cells as a cause for remyelination failure in chronic multiple sclerosis. Brain 2008; 131: 1749–58.

Lassmann H, Bruck W, Lucchinetti C, Rodriguez M. Remyelination in multiple sclerosis. Mult Scler 1997; 3: 133–6.

Lassmann H, Bruck W, Lucchinetti CF. The immunopathology of multiple sclerosis: an overview. Brain Pathol 2007; 17: 210–18.

Linington C, Engelhardt B, Kapocs G, Lassman H. Induction of persistently demyelinated lesions in the rat following the repeated adoptive transfer of encephalitogenic T cells and demyelinating antibody. J Neuroimmunol 1992; 40: 219–24.

Liu Z, Li Y, Zhang J, Elias S, Chopp M. Evaluation of corticospinal axon loss by fluorescent dye tracing in mice with experimental autoimmune encephalomyelitis. J Neurosci Methods 2008; 167: 191–7.

MacKenzie-Graham A, Tiwari-Woodruff SK, Sharma G, Aguilar C, Vo KT, Strickland LV, et al. Purkinje cell loss in experimental autoimmune encephalomyelitis. Neuroimage 2009; 48: 637–51.

Mallon BS, Shick HE, Kidd GJ, Macklin WB. Proteolipid promoter activity distinguishes two populations of NG2-positive cells throughout neonatal cortical development. J Neurosci 2002; 22: 876–85.

Manson SC, Palace J, Frank JA, Matthews PM. Loss of interhemispheric inhibition in patients with multiple sclerosis is related to corpus callosum atrophy. Exp Brain Res 2006; 174: 728–33.

Manson SC, Wegner C, Filippi M, Barkhof F, Beckmann C, Ciccarelli O, et al. Impairment of movement-associated brain deactivation in multiple sclerosis: further evidence for a functional pathology of interhemispheric neuronal inhibition. Exp Brain Res 2008; 187: 25–31.

Marin-Husstege M, Muggironi M, Raban D, Skoff RP, Casaccia-Bonnefil P. Oligodendrocyte progenitor proliferation and

maturation is differentially regulated by male and female sex steroid hormones. Dev Neurosci 2004; 26: 245–54.
McMorris FA, Smith TM, DeSalvo S, Furlanetto RW. Insulin-like growth factor I/somatomedin C: a potent inducer of oligodendrocyte development. Proc Natl Acad Sci USA 1986; 83: 822–6.
Meltser I, Tahera Y, Simpson E, Hultcrantz M, Charitidi K, Gustafsson JA, et al. Oestrogen receptor beta protects against acoustic trauma in mice. J Clin Invest 2008; 118: 1563–70.
Molyneux PD, Kappos L, Polman C, Pozzilli C, Barkhof F, Filippi M, et al. The effect of interferon beta-1b treatment on MRI measures of cerebral atrophy in secondary progressive multiple sclerosis. European Study Group on Interferon beta-1b in secondary progressive multiple sclerosis. Brain 2000; 123 (Pt 11): 2256–63.
Morales LB, Loo KK, Liu HB, Peterson C, Tiwari-Woodruff S, Voskuhl RR. Treatment with an oestrogen receptor alpha ligand is neuroprotective in experimental autoimmune encephalomyelitis. J Neurosci 2006; 26: 6823–33.
Narayanan SP, Flores AI, Wang F, Macklin WB. Akt signals through the mammalian target of rapamycin pathway to regulate CNS myelination. J Neurosci 2009; 29: 6860–70.
Ozturk A, Smith SA, Gordon-Lipkin EM, Harrison DM, Shiee N, Pham DL, et al. MRI of the corpus callosum in multiple sclerosis: association with disability. Mult Scler 16: 166–77.
Pagani E, Rocca MA, Gallo A, Rovaris M, Martinelli V, Comi G, et al. Regional brain atrophy evolves differently in patients with multiple sclerosis according to clinical phenotype. AJNR Am J Neuroradiol 2005; 26: 341–6.
Pang Y, Zheng B, Fan LW, Rhodes PG, Cai Z. IGF-1 protects oligodendrocyte progenitors against TNFalpha-induced damage by activation of PI3K/Akt and interruption of the mitochondrial apoptotic pathway. Glia 2007; 55: 1099–107.
Patrikios P, Stadelmann C, Kutzelnigg A, Rauschka H, Schmidbauer M, Laursen H, et al. Remyelination is extensive in a subset of multiple sclerosis patients. Brain 2006; 129: 3165–72.
Pelletier J, Suchet L, Witjas T, Habib M, Guttmann CR, Salamon G, et al. A longitudinal study of callosal atrophy and interhemispheric dysfunction in relapsing-remitting multiple sclerosis. Arch Neurol 2001; 58: 105–11.
Prineas JW, Connell F. Remyelination in multiple sclerosis. Ann Neurol 1979; 5: 22–31.
Quesada A, Lee BY, Micevych PE. PI3 kinase/Akt activation mediates oestrogen and IGF-1 nigral DA neuronal neuroprotection against a unilateral rat model of Parkinson's disease. Dev Neurobiol 2008; 68: 632–44.
Rasmussen S, Wang Y, Kivisakk P, Bronson RT, Meyer M, Imitola J, et al. Persistent activation of microglia is associated with neuronal dysfunction of callosal projecting pathways and multiple sclerosis-like lesions in relapsing–remitting experimental autoimmune encephalomyelitis. Brain 2007; 130: 2816–29.
Reeves TM, Phillips LL, Povlishock JT. Myelinated and unmyelinated axons of the corpus callosum differ in vulnerability and functional recovery following traumatic brain injury. Exp Neurol 2005; 196: 126–37.
Reynolds R, Cenci di Bello I, Dawson M, Levine J. The response of adult oligodendrocyte progenitors to demyelination in EAE. Prog Brain Res 2001; 132: 165–74.
Romanelli RJ, Mahajan KR, Fulmer CG, Wood TL. Insulin-like growth factor-I-stimulated Akt phosphorylation and oligodendrocyte progenitor cell survival require cholesterol-enriched membranes. J Neurosci Res 2009; 87: 3369–77.
Rossouw JE, Harlan WR. Postmenopausal oestrogen and the risk of breast cancer. The need for randomized trials. Ann Epidemiol 1994; 4: 255–6.
Singer W. Development and plasticity of cortical processing architectures. Science 1995; 270: 758–64.
Slaets H, Hendriks JJ, van den Haute C, Coun F, Baekelandt V, Stinissen P, et al. CNs-targeted lif expression improves therapeutic efficacy and limits autoimmune-mediated demyelination in a model of multiple sclerosis. Mol Ther 2010; 18: 684–91.
Sribnick EA, Wingrave JM, Matzelle DD, Wilford GG, Ray SK, Banik NL. Oestrogen attenuated markers of inflammation and decreased lesion volume in acute spinal cord injury in rats. J Neurosci Res 2005; 82: 283–93.
Steinman L, Zamvil SS. How to successfully apply animal studies in experimental allergic encephalomyelitis to research on multiple sclerosis. Ann Neurol 2006; 60: 12–21.
Takao T, Flint N, Lee L, Ying X, Merrill J, Chandross KJ. 17beta-estradiol protects oligodendrocytes from cytotoxicity induced cell death. J Neurochem 2004; 89: 660–73.
Tiwari-Woodruff S, Morales LB, Lee R, Voskuhl RR. Differential neuroprotective and antiinflammatory effects of oestrogen receptor (ER)alpha and ERbeta ligand treatment. Proc Natl Acad Sci U S A 2007; 104: 14813–18.
Tiwari-Woodruff S, Voskuhl RR. Neuroprotective and anti-inflammatory effects of oestrogen receptor ligand treatment in mice. J Neurol Sci 2009; 286: 81–5.
Trapp BD, Nave KA. Multiple sclerosis: an immune or neurodegenerative disorder? Annu Rev Neurosci 2008; 31: 247–69.
Trojano M, Russo P, Fuiani A, Paolicelli D, Di Monte E, Granieri E, et al. The Italian Multiple Sclerosis Database Network (MSDN): the risk of worsening according to IFNbeta exposure in multiple sclerosis. Mult Scler 2006; 12: 578–85.
Tyler WA, Gangoli N, Gokina P, Kim HA, Covey M, Levison SW, et al. Activation of the mammalian target of rapamycin (mTOR) is essential for oligodendrocyte differentiation. J Neurosci 2009; 29: 6367–78.
Van der Walt A, Butzkueven H, Kolbe S, Marriott M, Alexandrou E, Gresle M, et al. Neuroprotection in multiple sclerosis: A therapeutic challenge for the next decade. Pharmacol Ther 2010; 126: 82–93.
Wang M, Wang Y, Weil B, Abarbanell A, Herrmann J, Tan J, et al. Oestrogen receptor beta mediates increased activation of PI3K/Akt signaling and improved myocardial function in female hearts following acute ischemia. Am J Physiol Regul Integr Comp Physiol 2009; 296: R972–8.
Warlop NP, Fieremans E, Achten E, Debruyne J, Vingerhoets G. Callosal function in MS patients with mild and severe callosal damage as reflected by diffusion tensor imaging. Brain Res 2008; 1226: 218–25.
Waxman SG. Axonal conduction and injury in multiple sclerosis: the role of sodium channels. Nat Rev Neurosci 2006; 7: 932–41.
Wensky AK, Furtado GC, Marcondes MC, Chen S, Manfra D, Lira SA, et al. IFN-gamma determines distinct clinical outcomes in autoimmune encephalomyelitis. J Immunol 2005; 174: 1416–23.
Wilson ME, Dimayuga FO, Reed JL, Curry TE, Anderson CF, Nath A, et al. Immune modulation by oestrogens: role in CNS HIV-1 infection. Endocrine 2006; 29: 289–97.
Xu K, Xu Y, Brown-Jermyn D, Chen JF, Ascherio A, Dluzen DE, et al. Oestrogen prevents neuroprotection by caffeine in the mouse 1-methyl-4-phenyl-1,2,3,6-tetrahydropyridine model of Parkinson's disease. J Neurosci 2006; 26: 535–41.
Yue X, Lu M, Lancaster T, Cao P, Honda S, Staufenbiel M, et al. Brain oestrogen deficiency accelerates Abeta plaque formation in an Alzheimer's disease animal model. Proc Natl Acad Sci USA 2005; 102: 19198–203.
Zhang Z, Cerghet M, Mullins C, Williamson M, Bessert D, Skoff R. Comparison of in vivo and in vitro subcellular localization of oestrogen receptors alpha and beta in oligodendrocytes. J Neurochem 2004; 89: 674–84.
Zhu TS, Glaser M. Neuroprotection and enhancement of remyelination by estradiol and dexamethasone in cocultures of rat DRG neurons and Schwann cells. Brain Res 2008; 1206: 20–32.
Ziehn MO, Avedisian AA, Tiwari-Woodruff S, Voskuhl RR. Hippocampal CA1 atrophy and synaptic loss during experimental autoimmune encephalomyelitis, EAE. Lab Invest 2010; 90: 774–86.